

**Coulomb branch of  $\mathcal{N} = 4$  SYM and dilatonic scions in supergravity**Daniel Elander<sup>1</sup>,<sup>✉</sup> Maurizio Piai<sup>2</sup>,<sup>✉</sup> and John Roughley<sup>2</sup><sup>1</sup>*Laboratoire Charles Coulomb (L2C), University of Montpellier, CNRS, 34095 Montpellier, France*<sup>2</sup>*Department of Physics, College of Science, Swansea University, Singleton Park, Swansea SA2 8PP, Wales, United Kingdom* (Received 19 March 2021; accepted 24 June 2021; published 2 August 2021)

We find a parametrically light dilaton in special confining theories in three dimensions. Their duals form what we call a *scion* of solutions to the supergravity associated with the large- $N$  limit of the Coulomb branch of the  $\mathcal{N} = 4$  Super-Yang-Mills theory. The supergravity description contains one scalar with bulk mass that saturates the Breitenlohner-Freedman unitarity bound. The new solutions are defined within supergravity, they break supersymmetry and scale invariance, and one dimension is compactified on a shrinking circle, yet they are completely regular. An approximate dilaton appears in the spectrum of background fluctuations (or composite states in the confining theory), and becomes parametrically light along a metastable portion of the scion of new supergravity solutions, in close proximity of a tachyonic instability. A first-order phase transition separates stable backgrounds, for which the approximate dilaton is not parametrically light, from metastable and unstable backgrounds, for which the dilaton becomes parametrically light, and eventually tachyonic.

DOI: [10.1103/PhysRevD.104.046003](https://doi.org/10.1103/PhysRevD.104.046003)**I. INTRODUCTION**

In Refs. [1,2], we proposed a mechanism giving rise to an approximate dilaton in the spectrum of composite states of special classes of confining theories, in four dimensions, that admit a higher-dimensional gravity dual. We provided two explicit, calculable realizations of this mechanism, which generalizes the ideas proposed in Ref. [3] (and is further critically discussed in Refs. [4–6]). We considered non-anti-de Sitter (AdS) gravity backgrounds in proximity of classical instabilities—generalizing the proximity to the Breitenlohner-Freedman (BF) unitarity bound [7] in AdS space. An approximate dilaton (a scalar particle coupling to the trace of the energy-momentum tensor) emerges along special branches of supergravity solutions. Portions of the branches yield stable solutions, while complementary ones describe metastable or even unstable solutions. Moving in parameter space along the branch of solutions, the dilaton has finite mass for stable solutions, becomes parametrically light for metastable ones, and tachyonic for the unstable ones.

The analysis follows the prescriptions of gauge-gravity dualities [8–11], in the calculation of the free energy, via holographic renormalization [12–14], and of the spectrum

of the bound states, via a convenient gauge-invariant formalism [15–19]. We adopt the holographic description of confinement, the calculation of Wilson loops [20–26], and the interpretation of singularities [27]. We restrict attention to well established supergravity theories (top-down holography). Ref. [1] studies the half-maximal supergravity in  $D = 6$  dimensions, due to Romans [28–31] (see also Refs. [32–49]), compactified on a circle [50–53], while Ref. [2] considers the maximal supergravity in  $D = 7$  dimensions [54–58], compactified on a two-torus [59,60]. In Refs. [1,2], we explored regions of the admissible parameter space overlooked in the earlier literature.

The significance of Refs. [1,2] extends beyond producing calculable examples of the ideas exposed in Refs. [3–6]. Recent years saw a resurgence of interest in the literature on the dilaton effective field theory (EFT) description of near-conformal, strongly coupled systems in four dimensions (see for instance Refs. [61–73]). The literature on the subject has a long history [74], including early attempts to explain the long distance behavior of Yang-Mills [75] and walking technicolor [76–78] theories. One motivation for the revival is the uncovering of a light scalar particle, possibly a dilaton, in special  $SU(3)$  lattice gauge theories coupled to matter [79–90]. Previously, the study of simple bottom-up holographic models showed the emergence of a dilaton in special cases of theoretical relevance [91–105]. Even top-down holography provided supporting evidence for the existence of a light scalar in special confining theories [106–110] related to the conifold [111–117]. Furthermore, the distinctive features of the dilaton EFT

---

*Published by the American Physical Society under the terms of the Creative Commons Attribution 4.0 International license. Further distribution of this work must maintain attribution to the author(s) and the published article's title, journal citation, and DOI. Funded by SCOAP<sup>3</sup>.*

have been applied to phenomenological extensions of the standard model [118–129], including their use in the context of composite Nambu-Goldstone-Higgs models [130].

The gravity duals of the confining theories studied in Refs. [1,2] exhibit large departures from AdS geometry. What renders one of the scalar fluctuations parametrically light along the metastable branch is the interplay between the presence of a vacuum expectation value (VEV) breaking spontaneously scale invariance, the explicit breaking due to relevant deformations, and the effects of the nearby instability. The resulting scalar is an approximate dilaton, in the sense that it couples as expected to the trace of the energy-momentum tensor of the dual field theory; this is demonstrated by the failure of the probe approximation (which ignores the fluctuations of the trace of metric [131]) to reproduce correctly the mass spectrum. We refer the reader to the original publications for the details, and we defer commenting on potential phenomenological applications to extensions of the standard model and to Higgs physics [132,133].

The purpose of this paper is to exhibit a third example of this mechanism, but realized in a lower dimensional theory, in backgrounds that in the far UV approach an AdS geometry, with bulk scalar mass close to the BF bound. This hence highlights differences and similarities with other proposals for the origin of the dilaton. We study a particular truncation of the  $\mathcal{N} = 8$  maximal supergravity theory in  $D = 5$  dimensions, which is (loosely) associated with the Coulomb branch of  $\mathcal{N} = 4$  super-Yang-Mills (SYM) theories. By introducing a relevant deformation, and compactifying one dimension on a circle, we build a scion<sup>1</sup> of gravity backgrounds yielding a light dilaton and admitting an interpretation in terms of a field theory in three dimensions that confines. The scion provides a one-parameter family generalization of the gravity background occasionally denoted in the literature as  $\text{QCD}_3$ , and for which the spectrum of fluctuations is known [60].

The paper is organized as follows. We summarize in Sec. II the main features of the Coulomb branch, as well as the consistent truncation of maximal supergravity in  $D = 5$  dimensions, its reduction to  $D = 4$  dimensions, the lift to  $D = 10$  type IIB supergravity, and the prescription for Wilson loops. Section III summarizes the classes of solutions we investigate in this paper: we present the UV and IR expansions, then compute curvature invariants and Wilson loops to characterize the solutions. We compute the spectrum of fluctuations for the solutions in Sec. IV, in

<sup>1</sup>The dual of the Coulomb branch is sourced by a discrete distribution of displaced D3 branes; conversely the pure supergravity action and lift we borrow from the literature [134] leads to singular supersymmetric solutions. In view of this loose relation between supergravity theory and Coulomb branch, we refer to our new solutions, obtained by elaborating on the gravity theory, as forming a scion, rather than a branch, as a way to emphasize their hybrid nature.

the appropriate number of dimensions. In Sec. V we compare the free energies, to discuss the stability of the solutions. After the conclusions in Sec. VI, we supplement the material with Appendix A, summarizing known results for the supersymmetric solutions, and Appendix B, exhibiting asymptotic expansions of the fluctuations used in computing the spectra.

## II. THE MODEL

The  $\mathcal{N} = 8$  maximal supergravity in  $D = 5$  dimensions [135–137] has played a central role in the history of gauge-gravity dualities. It descends from dimensional reduction of type IIB supergravity in  $D = 10$  dimensions on the five-sphere  $S^5$  [138,139]. It has recently been established that this is a consistent truncation [140,141], and the full uplift back to type IIB is known [141–143] (see also Refs. [134,144,145]). The gauge symmetry is  $SO(6) \sim SU(4)$ —capturing the isometries of  $S^5$ , and the R-symmetry of the dual field theory, respectively. The field content includes 42 real scalars that match  $\mathcal{N} = 4$  field-theory operators on the basis of their transformation properties under  $SU(4)$ ; the complex singlet  $1_C$  corresponds to the holomorphic gauge coupling, the symmetric  $10_C$  to the fermion masses, and the real  $20'$  to the matrix of squared masses for the scalars  $X_i$ , with  $i = 1, \dots, 6$  (see e.g., Sec. 2.2.5 of Ref. [11], or the introduction of Ref. [146]).

One of the background solutions of  $D = 5$  maximal supergravity lifts in type IIB to the  $\text{AdS}_5 \times S^5$  background geometry providing the weakly-coupled dual description of  $\mathcal{N} = 4$  SYM with  $SU(N)$  gauge group, in the (decoupling) limit of large  $N$  and large 't Hooft coupling [8]. The supergravity solution is also the appropriate decoupling limit of the configuration sourced by a stack of  $N$  coincident D3 branes. Following Ref. [147] (see also Refs. [23,148,149]) we refer to the Coulomb branch as the space of inequivalent vacua of the  $\mathcal{N} = 4$  theory that preserves 16 supercharges. The space is so called because away from its  $SO(6)$ -invariant configuration the gauge group of the field theory is partially higgsed, and the massless gauge bosons mediate Coulomb interactions.

In the language of extended objects in  $D = 10$  dimensions, the literature identified multi-centred D3-brane solutions [23,147] with the moduli space of  $\mathcal{N} = 4$  SYM, in the sense that points of the Coulomb branch are associated with distributions of the  $N$  D3 branes over  $\mathbb{R}^6$  (conveniently parametrized as a cone over the sphere  $S^5$ ), accompanied by the higgsing of  $SU(N)$ . By taking  $N \rightarrow \infty$ , while introducing a continuous distribution of D3 branes, one might hope to recover a supergravity description of the Coulomb branch still within maximal  $\mathcal{N} = 8$  supergravity in  $D = 5$  dimensions. In fact, the resulting metrics satisfy the supergravity equations [147], but are singular (see for example the discussion after Eq. (3.12) of Ref. [150]). These solutions are captured by a consistent

truncation [134,144,145] that retains only the  $20'$  scalars, dual to the symmetric and traceless operator

$$20' \sim \left( \delta_i^k \delta_j^\ell - \frac{1}{6} \delta_{ij} \delta^{kl} \right) \text{Tr} X_k X_\ell. \quad (1)$$

There are five subclasses of solutions that preserve  $SO(n) \times SO(6-n)$  subgroups of  $SO(6)$ , with  $n = 1, \dots, 5$  [147]. With abuse of language, the supersymmetric backgrounds of this type are referred to as the Coulomb branch, though such solutions are singular, and hence incomplete as gravity duals.

We further restrict our attention to the  $n = 2$  and the  $n = 4$  cases [23]. The spectrum of the  $n = 2$  case is quite peculiar: both the spin-zero and spin-two spectra have a gap and a cut opening above a finite value [12,147,151–154] (see also Refs. [154,155] for the spectra of vectors). The choices  $n = 2, 4$  are convenient also because they are both captured by one of the subtruncations of the theory in Ref. [156]—which retains only two scalars, one in the  $20'$  and the  $10_C$ , respectively (see also the discussions in Refs. [157,158]). Setting to zero the latter of the two scalars reduces the field content to just one scalar ( $\phi$  in our notation), and the lift to  $D = 10$  dimensions is comparatively simple.

The gravity descriptions for  $n = 2, 4$  are different;  $n$  is associated with the ball  $\mathcal{B}^n$  inside the internal space (including the radial direction) over which one distributes the  $N$  D3 branes, and is then reflected in the Ramond fluxes in supergravity. We will identify two distinct classes of solutions to the supergravity equations, distinguished by the negative or positive sign of  $\phi$  at the end of space, which we associate with  $n = 2, 4$ , respectively (see also the discussion at the end of Sec. 2 in Ref. [134]). We display the supersymmetric solutions and summarize their known properties in Appendix A.

We reconsider the system consisting of the scalar  $\phi$  coupled to gravity in  $D = 5$  dimensions, and describe more general classes of solutions with respect to the literature. These more general deformations break explicit supersymmetry and scale invariance, hence lifting the space of vacua, and modifying the spectrum of the theory. We focus on solutions that involve either of two possibilities.

(a) In Secs. III B and III C, we display singular domain wall solutions that generalize the supersymmetric ones while preserving Poincaré invariance in four dimensions. The dual field theory is deformed by mass terms, breaking supersymmetry, R-symmetry, and scale invariance. We compute the spectrum of fluctuations—which barring the singularity would be interpreted as bound states of the dual field theory in four dimensions—and the behavior of the quark-antiquark potential between static sources, generalizing the results of Ref. [23]. We discover one new special subclass of mildly singular solutions, that yield a long-

distance potential  $E_W \propto 1/L^2$  persisting up to infinite separation  $L$ .

(b) In Sec. III D, we identify background solutions for which one of the dimensions of the external space-time is compactified on a circle, which shrinks smoothly to zero size at some finite value of the radial (holographic) direction. These are regular solutions, and the dual field theory yields linear confinement in three dimensions, as explicitly shown by the Wilson loops. We compute the spectrum of fluctuations, generalizing the results of Ref. [60], and discover new features, such as the emergence of an approximate dilaton.

### A. Sigma-model in $D = 5$ dimensions

We denote with hatted symbols quantities characterizing the theory in  $D = 5$  dimensions. The action of the canonically normalized scalar  $\phi$  coupled to gravity is the following (in the notation of Ref. [131]):

$$\mathcal{S}_5 = \int d^5x \sqrt{-\hat{g}_5} \left( \frac{\hat{\mathcal{R}}_5}{4} - \frac{1}{2} \hat{g}^{\hat{M}\hat{N}} \partial_{\hat{M}} \phi \partial_{\hat{N}} \phi - \mathcal{V}_5 \right). \quad (2)$$

Here  $\hat{g}_5$  is the determinant of the metric,  $\hat{g}^{\hat{M}\hat{N}}$  its inverse, and  $\hat{\mathcal{R}}_5$  the Ricci scalar, while  $\mathcal{V}_5$  is the potential.

The domain wall (DW) solutions manifestly preserve Poincaré invariance in four dimensions. They can be obtained by adopting the following ansatz for the metric,

$$ds_{\text{DW}}^2 = e^{2\mathcal{A}(\rho)} dx_{1,3}^2 + d\rho^2. \quad (3)$$

By assumption, the only nontrivial functions determining the background are  $\mathcal{A}(\rho)$  and  $\phi(\rho)$ , with no dependence on other coordinates. The resulting second-order equations of motion are the following:

$$0 = \partial_\rho^2 \phi + 4\partial_\rho \mathcal{A} \partial_\rho \phi - \partial_\phi \mathcal{V}_5, \quad (4)$$

$$0 = 4(\partial_\rho \mathcal{A})^2 + \partial_\rho^2 \mathcal{A} + \frac{4}{3} \mathcal{V}_5, \quad (5)$$

$$0 = 6(\partial_\rho \mathcal{A})^2 - \partial_\rho \phi \partial_\rho \phi + 2\mathcal{V}_5. \quad (6)$$

The conventions we are using [16] in writing the action in Eq. (2) are such that if the potential  $\mathcal{V}_5$  of the model can be written in terms of a superpotential  $\mathcal{W}$  satisfying

$$\mathcal{V}_5 = \frac{1}{2} (\partial_\phi \mathcal{W})^2 - \frac{4}{3} \mathcal{W}^2, \quad (7)$$

for the metric ansatz  $ds_{\text{DW}}^2$ , then the solutions to the first-order equations

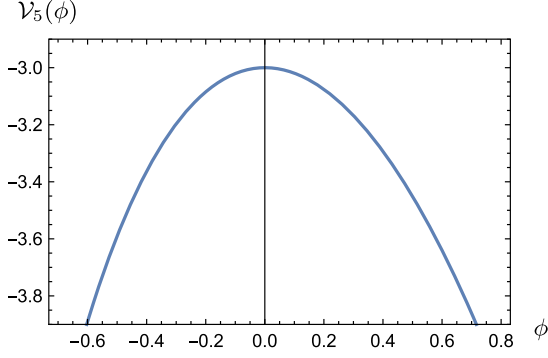


FIG. 1. The potential  $\mathcal{V}_5$  in Eq. (10) for the sigma-model in  $D = 5$  dimensions, as a function of the scalar  $\phi$ .

$$\partial_\rho \mathcal{A} = -\frac{2}{3} \mathcal{W} \quad \text{and} \quad \partial_\rho \phi = \partial_\phi \mathcal{W}, \quad (8)$$

are also solutions to the second-order Eqs. (4)–(6).

The superpotential is the following [12,147,151,152]:

$$\mathcal{W} = -e^{-\frac{2\phi}{\sqrt{6}}} - \frac{1}{2} e^{\frac{4\phi}{\sqrt{6}}}, \quad (9)$$

and admits an exact AdS<sub>5</sub> solution with unit scale. The potential is given by

$$\mathcal{V}_5(\phi) = -e^{-\frac{4\phi}{\sqrt{6}}} - 2e^{\frac{2\phi}{\sqrt{6}}}, \quad (10)$$

and is depicted in Fig. 1.

The first-order equations admit solutions that yield a departure from AdS<sub>5</sub> in the interior of the geometry, which may correspond to  $n = 2$  (D3 branes distributed on  $\mathcal{B}^2$ ) or  $n = 4$  (D3 branes distributed on  $\mathcal{B}^4$ ). For small  $\phi$  one finds that  $\mathcal{W} \simeq -\frac{3}{2} - \phi^2 + \dots$ , hence these solutions are interpreted in terms the VEV of an operator of dimension  $\Delta = 2$  in the dual field theory. This saturates the BF bound and, with respect to Refs. [1,2], brings this study in closer contact with the arguments in Ref. [3].

### B. Reduction to $D = 4$ dimensions

We want to model a confining dual field theory in three dimensions. Following Ref. [59], we therefore assume that one spatial dimension is a circle, the size of which may depend on the radial direction parametrized by  $\rho$  in the five-dimensional geometry, and we hence allow for the breaking of four-dimensional Poincaré invariance.

Regular background solutions in which the size of the circle shrinks smoothly to zero (at some finite value of the radial direction  $\rho = \rho_o$ ) introduce a mass gap in the (lower-dimensional) dual field theory, and exhibit the physics of confinement—we discuss how in Secs. III C and III D.

We elect to describe the geometry by applying dimensional reduction of the gravity theory to four dimensions, with the introduction of a new dynamical scalar that encodes the size of the circle. In the remainder of this

subsection we provide the technical details of the construction.

We reduce to  $D = 4$  dimensions by adopting the following ansatz, as in Refs. [131,52]:

$$ds_5^2 = e^{-2\chi(r)} ds_4^2 + e^{4\chi(r)} d\eta^2, \quad (11)$$

where the angle  $0 \leq \eta < 2\pi$  parametrises a circle, the four-dimensional metric takes the domain wall form

$$ds_4^2 = e^{2A(r)} dx_{1,2}^2 + dr^2, \quad (12)$$

and the new background scalar  $\chi(r)$  and warp factor  $A(r)$  depend only on the new radial coordinate  $r$ .

The action in  $D = 4$  dimensions is

$$\mathcal{S}_4 = \int d^4x \sqrt{-g_4} \left[ \frac{\mathcal{R}_4}{4} - \frac{g^{MN}}{2} G_{ab} \partial_M \Phi^a \partial_N \Phi^b - \mathcal{V}_4 \right], \quad (13)$$

where the sigma-model metric for the scalar fields  $\Phi^a = \{\phi, \chi\}$  is  $G_{ab} = \text{diag}(1, 3)$ , and the potential is

$$\mathcal{V}_4 = e^{-2\chi} \mathcal{V}_5. \quad (14)$$

We explicitly verified that  $\mathcal{S}_5 = \int d\eta (\mathcal{S}_4 + \partial \mathcal{S})$ , where

$$\partial \mathcal{S} = \int d^4x \partial_M \left( \frac{1}{2} \sqrt{-g_4} g^{MN} \partial_N \chi \right). \quad (15)$$

After the change of variables  $\partial_r = e^{-\chi} \partial_\rho$ , the equations of motion for the background read as follows:

$$0 = \partial_\rho \phi (3\partial_\rho A - \partial_\rho \chi) + \partial_\rho^2 \phi + \sqrt{\frac{8}{3}} e^{-\sqrt{\frac{8}{3}}\phi} [e^{\sqrt{6}\phi} - 1], \quad (16)$$

$$0 = 3\partial_\rho A \partial_\rho \chi - \partial_\rho \chi^2 + \partial_\rho^2 \chi - \frac{2}{3} e^{-\sqrt{\frac{8}{3}}\phi} [2e^{\sqrt{6}\phi} + 1], \quad (17)$$

$$0 = \partial_\rho A \partial_\rho \chi - 3\partial_\rho A^2 - \partial_\rho^2 A + 2e^{-\sqrt{\frac{8}{3}}\phi} [2e^{\sqrt{6}\phi} + 1], \quad (18)$$

$$0 = 3\partial_\rho A^2 - 3\partial_\rho \chi^2 - \partial_\rho \phi^2 - 2e^{-\sqrt{\frac{8}{3}}\phi} [2e^{\sqrt{6}\phi} + 1]. \quad (19)$$

By combining Eqs. (17) and (18), we obtain

$$\partial_\rho [e^{3A-\chi} (3\partial_\rho \chi - \partial_\rho A)] = 0, \quad (20)$$

which defines a conserved quantity along the flow in  $\rho$ .

### C. Lift to type IIB in $D = 10$ dimensions

We take the lift to type IIB supergravity in  $D = 10$  dimensions from Ref. [134]. The dilaton/axion subsystem is trivial (see Sec. 3.2 of Ref. [134]), and there is no distinction between Einstein and string frames.

We parametrize the five-sphere  $S^5$  in terms of five angles  $0 \leq \theta \leq \pi/2$ ,  $0 \leq \tilde{\theta} \leq \pi$ ,  $0 \leq \varphi, \tilde{\varphi} < 2\pi$ , and  $0 \leq \psi \leq 4\pi$ . The  $SU(2)$  left-invariant two-forms are

$$\sigma_1 = \cos \psi d\tilde{\theta} + \sin \psi \sin \tilde{\theta} d\tilde{\varphi}, \quad (21)$$

$$\sigma_2 = \sin \psi d\tilde{\theta} - \cos \psi \sin \tilde{\theta} d\tilde{\varphi}, \quad (22)$$

$$\sigma_3 = d\psi + \cos \tilde{\theta} d\tilde{\varphi}, \quad (23)$$

normalized according to  $d\sigma_i = \frac{1}{2} \sum_{jk} \epsilon_{ijk} \sigma_j \wedge \sigma_k$ .<sup>2</sup> We write the metric of the  $S^3$  as  $d\Omega_3^2 \equiv \frac{1}{4} \sum_{i=1}^3 \sigma_i^2$ , or

$$d\Omega_3^2 = \frac{1}{4} [d\tilde{\theta}^2 + \sin^2 \tilde{\theta} d\tilde{\varphi}^2 + (d\psi + d\tilde{\varphi} \cos \tilde{\theta})^2]. \quad (24)$$

We then follow Ref. [134] (see also Ref. [159]), with the following identifications: we set the two scalars  $\{\alpha, \chi\}$  of Ref. [134] to  $\alpha \equiv \phi/\sqrt{6}$  and  $\chi = 0$  (not to be confused with  $\chi$  in this paper), we set the coupling  $g = 2$ , and the normalization in Eq. (3.14) of Ref. [134] to  $a^2 = 2$ . The metric in  $D = 10$  dimensions is

$$ds_{10}^2 = \Omega^2 ds_5^2 + d\tilde{\Omega}_5^2, \quad (25)$$

where  $ds_5^2$  has been introduced in Eq. (11), while

$$d\tilde{\Omega}_5^2 = \frac{X^{1/2}}{\tilde{\rho}^3} \left( d\theta^2 + \frac{\tilde{\rho}^6}{X} \cos^2 \theta d\Omega_3^2 + \sin^2 \theta \frac{d\varphi^2}{X} \right). \quad (26)$$

The warp factor in the lift depends on  $\rho$  and  $\theta$ , because

$$\Omega^2 \equiv \frac{X^{1/2}}{\tilde{\rho}}, \quad (27)$$

where the functions determining the backgrounds are

$$\tilde{\rho} \equiv e^{\phi/\sqrt{6}}, \quad (28)$$

$$X \equiv \cos^2 \theta + \tilde{\rho}^6 \sin^2 \theta. \quad (29)$$

For  $\phi = 0$  one has  $\tilde{\rho} = 1 = X$ , and recovers the round  $S^5$ . The isometries associated with  $d\Omega_3^2$  and  $d\varphi^2$  match the  $SO(4)$  and  $SO(2)$  symmetries of the field theory.

By making use of the equations of motions for the scalars  $\phi$  and  $\chi$  and for the function  $A$ , we find that  $\mathcal{R}_{10} = 0$  identically. Yet, other invariants, such as the square of the Ricci and Riemann tensors, are nontrivial.

#### D. Rectangular Wilson loops

The expectation value of rectangular Wilson loops of sizes  $L$  and  $T$  in space and time, respectively, is computed using the standard holographic prescription [20,21] (see also Refs. [22–24]). Open strings, with extrema bound to the contour of the loop on the boundary of the space at  $\rho = +\infty$ , explore the geometry down to the turning point

<sup>2</sup>Compared to Ref. [134], we have  $\sigma_i$  (here) =  $2\sigma_i$  (Ref. [134]).

$\hat{\rho}_o$  in the holographic direction, and the problem reduces to a minimal surface one. The warp factor  $\Omega^2$  depends on  $\theta$ , but we restrict attention to configurations with  $\theta$  held fixed, and focus on the limiting cases  $\theta = 0$  and  $\theta = \pi/2$ . Taking  $T \rightarrow +\infty$ , we obtain the effective potential between static quarks as a function of the separation  $L$  between end-points of the string.

The calculation of the Wilson loop can proceed along the lines of the prescription in Refs. [22–26]. Starting from the elements of the metric in  $D = 10$  dimensions,  $ds^2 = g_{tt} dt^2 + g_{xx} dx^2 + g_{\rho\rho} d\rho^2 + \dots$ , we introduce the functions  $F^2(\rho, \theta) \equiv -g_{tt} g_{xx}$  and  $G^2(\rho, \theta) \equiv -g_{tt} g_{\rho\rho}$ , and the convenient quantity

$$V_{\text{eff}}^2(\rho, \hat{\rho}_o) \equiv \frac{F^2(\rho)}{F^2(\hat{\rho}_o) G^2(\rho)} (F^2(\rho) - F^2(\hat{\rho}_o)), \quad (30)$$

where the dependence on (constant)  $\theta$  is implicit. The separation between the end points of the string is

$$L(\hat{\rho}_o) = 2 \int_{\hat{\rho}_o}^{\infty} d\rho \frac{1}{V_{\text{eff}}(\rho, \hat{\rho}_o)}, \quad (31)$$

and the profile of the string in the  $(\rho, x)$ -plane is

$$x(\rho) = \begin{cases} \int_{\rho}^{\infty} \frac{dy}{V_{\text{eff}}(y, \hat{\rho}_o)}, & x < L(\hat{\rho}_o)/2, \\ L(\hat{\rho}_o) - \int_{\rho}^{\infty} \frac{dy}{V_{\text{eff}}(y, \hat{\rho}_o)}, & x > L(\hat{\rho}_o)/2. \end{cases} \quad (32)$$

The energy of the resulting configuration is

$$E(\hat{\rho}_o) = 2\kappa \int_{\hat{\rho}_o}^{\infty} d\rho \sqrt{\frac{F^2(\rho) G^2(\rho)}{F^2(\rho) - F^2(\hat{\rho}_o)}}. \quad (33)$$

As  $g_{xx} = -g_{tt} = \Omega^2 e^{2A-2\chi}$  and  $g_{\rho\rho} = \Omega^2$ , we find the  $\theta$ -dependent functions  $F^2(\rho, \theta) = X \tilde{\rho}^{-2} e^{4A-4\chi}$  and  $G^2(\rho, \theta) = X \tilde{\rho}^{-2} e^{2A-2\chi}$ , also written explicitly as

$$F^2(\rho, \theta) = (\cos^2 \theta + e^{\sqrt{6}\phi} \sin^2 \theta) e^{4A-4\chi-2\phi/\sqrt{6}}, \quad (34)$$

$$G^2(\rho, \theta) = (\cos^2 \theta + e^{\sqrt{6}\phi} \sin^2 \theta) e^{2A-2\chi-2\phi/\sqrt{6}}. \quad (35)$$

Eq. (33) is UV divergent, requiring the introduction of  $\rho_{\Lambda}$  as a UV cutoff, and to define the regulated  $E_{\Lambda}(\hat{\rho}_o)$  by restricting the range of integration. We define the following:

$$\Delta E_{\Lambda, \theta} \equiv 2\kappa \int_{\rho_o}^{\rho_{\Lambda}} d\rho G(\rho, \theta), \quad (36)$$

where the integral extends all the way to the end of space  $\rho_o$ , choose the case  $\theta = 0$  as a counterterm, and finally define the renormalized energy as

$$E_W(\hat{\rho}_o) \equiv \lim_{\rho_\Lambda \rightarrow +\infty} (E_\Lambda(\hat{\rho}_o) - \Delta E_{\Lambda,0}). \quad (37)$$

In confining theories, at large separations  $L(\hat{\rho}_o)$  the energy grows linearly and the string tension is given by

$$\sigma_{\text{eff}} \equiv \lim_{\hat{\rho}_o \rightarrow \rho_o} \frac{dE_W(\hat{\rho}_o)}{dL(\hat{\rho}_o)} = F(\rho_o). \quad (38)$$

A limiting configuration consists of two straight rods at distance  $L$ , both with fixed  $\theta$ , extending from the boundary to the end of space, connected by a straight portion of string at  $\hat{\rho}_o = \rho_o$ . Its energy is  $E_\theta = \Delta E_{\Lambda,\theta} - \Delta E_{\Lambda,0} + F(\rho_o, \theta)L$ . If  $F(\rho_o, \theta)$  vanishes, this configuration is indistinguishable from two disconnected ones, yielding screening in the dual theory—barring the caveats discussed in Ref. [160]. We set the normalization  $\kappa = 1$  from here on. There may be cases in which this procedure shows the emergence of a phase transition for the theory living on the probe [23] (see also the discussions in Refs. [26,161]).

### III. BACKGROUND SOLUTIONS

We classify in this section the background solutions we are interested in. We present their UV and IR expansions, and discuss curvature invariants and Wilson loops.

#### A. UV expansions

All the solutions of interest have the same asymptotic UV expansion, and they all correspond to deformations of the same dual theory. We expand them for  $z = e^{-\rho} \ll 1$ .

$$\begin{aligned} \phi(z) &= z^2 \phi_2 + z^2 \phi_{2l} \log(z) \\ &\quad + \frac{\sqrt{6}}{12} z^4 (2\phi_2^2 - 4\phi_2 \phi_{2l} + 3\phi_{2l}^2) \\ &\quad + \frac{\sqrt{6}}{3} z^4 \log(z) (\phi_2 \phi_{2l} - \phi_{2l}^2) \\ &\quad + \frac{z^4 \phi_{2l}^2 \log^2(z)}{\sqrt{6}} + \mathcal{O}(z^6), \end{aligned} \quad (39)$$

$$\begin{aligned} \chi(z) &= \chi_U - \frac{\log(z)}{2} + \chi_4 z^4 - \frac{1}{6} z^4 \phi_2 \phi_{2l} \log(z) \\ &\quad - \frac{1}{12} z^4 \phi_{2l}^2 \log^2(z) + \mathcal{O}(z^6), \end{aligned} \quad (40)$$

$$\begin{aligned} A(z) &= A_U - \frac{3 \log(z)}{2} - \frac{1}{2} z^4 \phi_2 \phi_{2l} \log(z) \\ &\quad + z^4 \left( \frac{\chi_4}{3} - \frac{1}{36} (8\phi_2^2 + \phi_{2l}^2) \right) \\ &\quad - \frac{1}{4} z^4 \phi_{2l}^2 \log^2(z) + \mathcal{O}(z^6). \end{aligned} \quad (41)$$

The integration constant  $A_U$  can be reabsorbed and set to zero, while  $\chi_U$  can be removed by a shift of radial

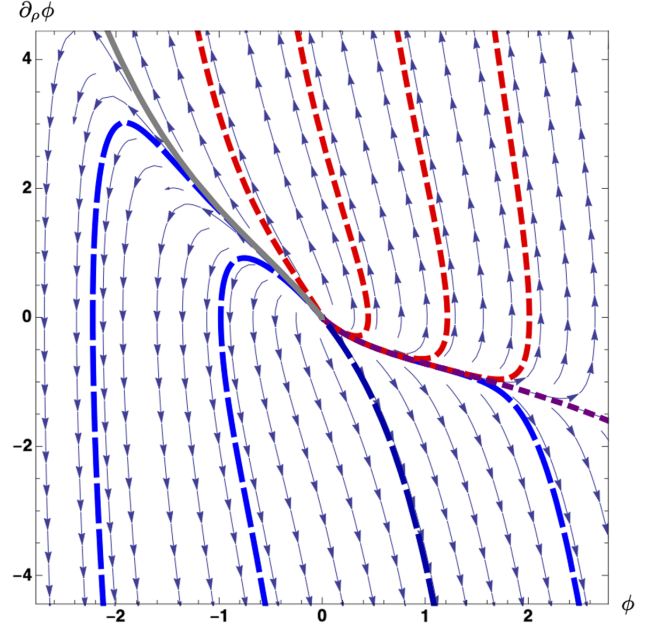


FIG. 2. Stream plot of the DW solutions departing from the trivial fixed point at  $(\phi, \partial_\rho \phi) = (0, 0)$ . The dashed (red) solutions are examples of the negative DW family described by the IR expansions in Eqs. (43) and (44). The long-dashed (blue) solutions are examples of the positive DW family with IR expansions in Eqs. (46) and (47); the case of the supersymmetric solution in Eqs. (A5) and (A6) is denoted by a darker shade of blue. The two special solutions are depicted by the continuous thick (gray) line—for the case of the supersymmetric solution in Eqs. (A3) and (A4), or Eqs. (A7) and (A8)—and the short-dashed (purple) line for the case described by Eqs. (49) and (50).

coordinate  $\rho$ .  $\phi_2$  is associated with the VEV of the aforementioned dimension-two operator of the dual field theory, and  $\phi_{2l}$  with its (supersymmetry-breaking) coupling. The parameter  $\chi_4$  is associated with the VEV of a dimension-four operator which triggers confinement.

Domain wall solutions in  $D = 5$  dimensions are recovered (locally) for  $\mathcal{A} = A - \chi = 2\chi$ , yielding two constraints on the five parameters of a generic solution,

$$A_U = 3\chi_U, \quad \chi_4 = -\frac{1}{96} (8\phi_2^2 + \phi_{2l}^2). \quad (42)$$

We illustrate the behavior of the singular DW solutions with the comprehensive catalogue in Fig. 2. We devote to them Secs. III B and III C (and Appendix A), before discussing in Sec. III D the scion of regular solutions corresponding to confining theories in three dimensions.

#### B. The negative DW family

The DW solutions for which  $\phi$  diverges to  $-\infty$  at the end of space generalise the  $n = 2$  supersymmetric case—see the dashed (red) lines in Fig. 2. The background functions, evaluated near the end of space  $\rho_o$ , are

$$\begin{aligned} \phi_-(\rho) &= \phi_o + \frac{1}{2} \sqrt{\frac{3}{2}} \log(\rho - \rho_o) \\ &\quad + \frac{4}{9} \sqrt{\frac{2}{3}} (\rho - \rho_o)^2 e^{-4\sqrt{\frac{2}{3}}\phi_o} + \dots, \end{aligned} \quad (43)$$

$$\begin{aligned} \mathcal{A}_-(\rho) &= \mathcal{A}_I + \frac{\log(\rho - \rho_o)}{4} \\ &\quad + \frac{2}{3} (\rho - \rho_o) e^{-2\sqrt{\frac{2}{3}}\phi_o} + \dots. \end{aligned} \quad (44)$$

Ignoring the inconsequential constants  $\mathcal{A}_I$  and  $\rho_o$ , this one-parameter family of solutions is labeled by the free parameter  $\phi_o$ . The curvature invariants of the gravity formulation in  $D = 5$  dimensions diverge; lifting to  $D = 10$  dimensions, the singular behavior first appears in

$$\mathcal{R}_{10, \hat{M} \hat{N}} \mathcal{R}_{10}^{\hat{M} \hat{N}} = \frac{10 e^{-\sqrt{6}\phi_o}}{\cos^2(\theta) (\rho - \rho_o)^{3/2}} + \dots, \quad (45)$$

A special limiting case (corresponding to  $\phi_o \rightarrow -\infty$ ) of the (singular) negative DW solutions is represented by the

thick (gray) line in Fig. 2, and is given by the IR expansions in Eqs. (A7) and (A8). It satisfies the first-order equations, as it coincides with the supersymmetric solutions  $(\phi_2, \mathcal{A}_2)$  described by Eqs. (A3) and (A4)—the solution corresponding to the ( $n = 2$ ) case of D3 branes distributed on a disk ( $\mathcal{B}^2$ ).

The study of the Wilson loops is exemplified in Fig. 3. The top-left panel depicts the case of backgrounds  $(\phi_-, \mathcal{A}_-)$  with  $\phi_o = -1$ . The string is tensionless at the end of space, as  $\lim_{\rho \rightarrow \rho_o} F^2(\rho) = 0$  for both choices  $\theta = 0, \pi/2$ . The separation  $L$  converges to zero for strings with end points at  $\rho = +\infty$ , when the turning point of the string configuration reaches the end of space, yielding the description of a phase transition such that the Wilson loop mimics screening at large  $L$ .

### C. The positive DW family

In the stream plot in Fig. 2, the long-dashed (blue) lines are examples of DW solutions in which the scalar  $\phi$  diverges to  $\phi \rightarrow +\infty$  at the end of space. Their IR expansions are

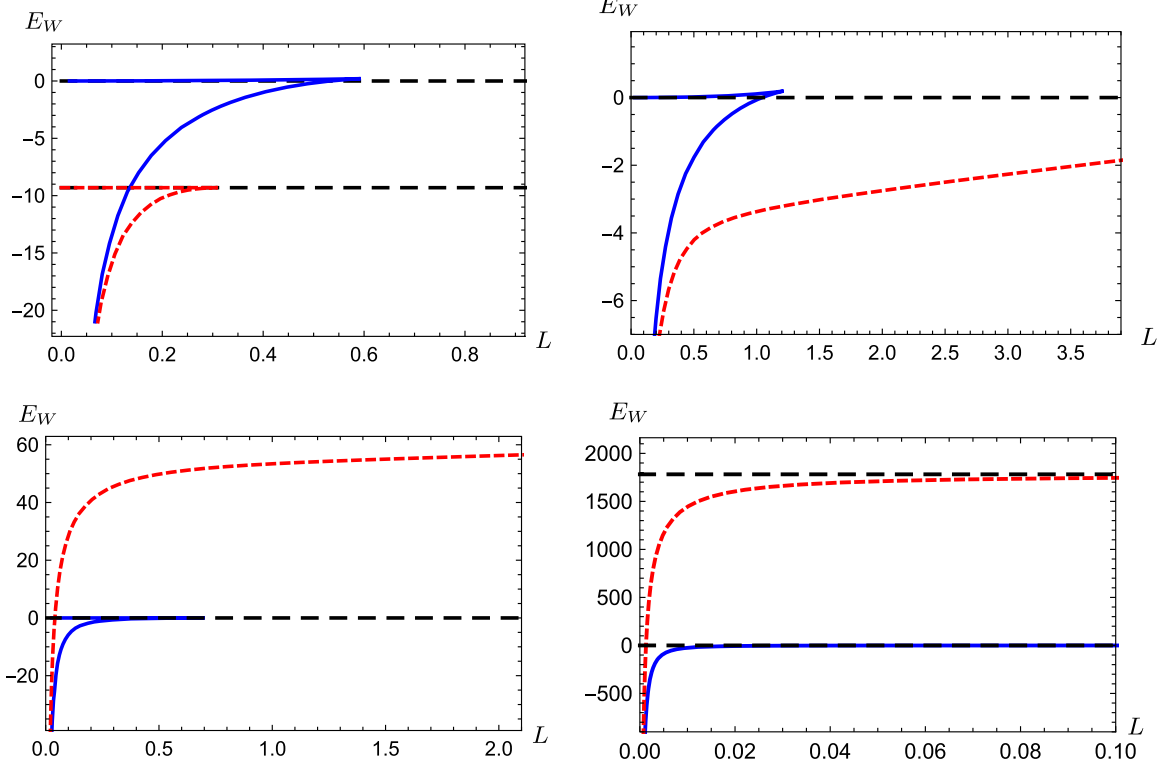


FIG. 3. Energy  $E_W$  as a function of the separation  $L$  in space, computed with rectangular Wilson loops by applying the prescription of gauge-gravity dualities, for four different backgrounds belonging to classes of nonsupersymmetric DW solutions chosen to have  $\mathcal{A}_I = 0$ . Left to right, and top to bottom, the panels show the results for the following backgrounds: the  $(\phi_-, \mathcal{A}_-)$  solution with  $\phi_o = -1$ , the  $(\phi_+, \mathcal{A}_+)$  solution with  $\phi_o = -1$ , the  $(\phi_+, \mathcal{A}_+)$  solution with  $\phi_o = +1$ , and the special  $(\phi_\infty, \mathcal{A}_\infty)$  solution corresponding to  $\phi_o \rightarrow +\infty$ . The horizontal long-dashed (black) lines denote string configurations sitting at the end of space, the continuous (blue) lines depict configurations with  $\theta = 0$ , and the short-dashed (red) lines represent configurations with  $\theta = \pi/2$ .

$$\begin{aligned} \phi_+(\rho) &= \phi_o - \frac{1}{2} \sqrt{\frac{3}{2}} \log(\rho - \rho_o) \\ &+ \frac{8}{15} \sqrt{\frac{2}{3}} e^{\sqrt{\frac{2}{3}} \phi_o} (\rho - \rho_o)^{3/2} + \dots, \end{aligned} \quad (46)$$

$$\begin{aligned} \mathcal{A}_+(\rho) &= \mathcal{A}_I + \frac{\log(\rho - \rho_o)}{4} \\ &+ \frac{32}{45} (\rho - \rho_o)^{3/2} e^{\sqrt{\frac{2}{3}} \phi_o} + \dots. \end{aligned} \quad (47)$$

These solutions generalize the supersymmetric one denoted  $(\phi_4, \mathcal{A}_4)$  in Eqs. (A5) and (A6)—the solutions corresponding to the  $(n = 4)$  case of D3 branes distributed on  $\mathcal{B}^4$ —to a one-parameter family, labeled by  $\phi_o$ . The supersymmetric case is recovered with the choice  $\phi_o = -\frac{1}{2} \sqrt{\frac{3}{2}} \log(\frac{4}{3})$ , and is highlighted by a darker long-dashed line in Fig. 2.

The five-dimensional curvature invariants diverge. In  $D = 10$  dimensions the divergence appears in

$$\mathcal{R}_{10, \hat{M} \hat{N}} \mathcal{R}_{10}^{\hat{M} \hat{N}} = \frac{405 e^{-8 \sqrt{\frac{2}{3}} \phi_o} \sin^4(2\theta)}{2048 \sin^{10}(\theta)} + \dots \quad (48)$$

The limit  $\theta \rightarrow 0$  is singular at the end of space, even in the case of the supersymmetric solution—see also Eq. (A12) and the discussion that follows it.

The calculation of the Wilson loops is exemplified in the top-right and bottom-left panels in Fig. 3, for  $\phi_o = -1$  and  $\phi_o = +1$ , respectively. For  $\theta = 0$ , once more  $\lim_{\rho \rightarrow \rho_o} F^2(\rho) = 0$ . The separation  $L$  vanishes when the turning point of the string configuration reaches the end of space, as we found for  $(\phi_-, \mathcal{A}_-)$ . But in the case  $\theta = \pi/2$ , we find that  $\lim_{\rho \rightarrow \rho_o} F^2(\rho) = \sigma^2 > 0$  is finite. The separation  $L$  diverges, and one recovers the linear potential  $E_W \simeq \sigma L$ .

When  $\phi_o < -\frac{1}{2} \sqrt{\frac{3}{2}} \log(\frac{4}{3})$ , the assumption of keeping  $\theta$  fixed fails, as at small  $L$  the configurations with  $\theta = \pi/2$  have lower energy than those with  $\theta = 0$ , while at large  $L$  the converse is true.

### 1. Special positive DW solutions

A limiting case of the positive DW solutions is depicted by the short-dashed (purple) line in Fig. 2. The IR expansions are

$$\begin{aligned} \phi_\infty(\rho) &= \sqrt{\frac{3}{2}} \log\left(\frac{45}{2}\right) - \sqrt{6} \log(\rho - \rho_o) \\ &+ \frac{2\sqrt{2}}{59535\sqrt{3}} (\rho - \rho_o)^6 + \dots, \end{aligned} \quad (49)$$

$$\begin{aligned} \mathcal{A}_\infty(\rho) &= \mathcal{A}_I + 4 \log(\rho - \rho_o) \\ &+ \frac{16}{893025} (\rho - \rho_o)^6 + \dots. \end{aligned} \quad (50)$$

The only parameters are the inconsequential  $\mathcal{A}_I$  and  $\rho_o$ . The five-dimensional curvature invariants diverge, but the lift to  $D = 10$  dimensions yields

$$\mathcal{R}_{10} = 0 = \lim_{\rho \rightarrow \rho_o} \mathcal{R}_{10, \hat{M} \hat{N}} \mathcal{R}_{10}^{\hat{M} \hat{N}}. \quad (51)$$

Yet, these solutions are singular as well, as illustrated by the simultaneous limits  $\rho \rightarrow \rho_o$  and  $\theta \rightarrow 0$  of the square of the Riemann tensor,

$$\lim_{\rho \rightarrow \rho_o} (\mathcal{R}_{10, \hat{M} \hat{N}} \mathcal{R}_{10}^{\hat{M} \hat{N}})^2 = \frac{9(15 + 10 \sin^2(\theta) + 7 \sin^4(\theta))}{5 \sin^6(\theta)}. \quad (52)$$

These solutions are the limiting case  $\phi_o \rightarrow +\infty$  of the  $(\phi_+, \mathcal{A}_+)$  general class, and the bottom-right panel in Fig. 3 shows a peculiarly interesting behavior for the quark-antiquark potential. The separation  $L$  is unbounded, the potential vanishes for  $L \rightarrow +\infty$ , and so does the string tension. We find the potential  $E_W \simeq -e^{1/6}/L$  at short  $L$ , and  $E_W \simeq -e^6/L^2$  at large  $L$  (for  $\mathcal{A}_I = 0$ ).

While the results of the study of the Wilson loops for the DW solutions are very suggestive, with the emergence of screening, confining, several types of Coulombic potentials and phase transitions, they must be all taken with caution; all the background solutions discussed so far (and in Appendix A) are singular. Hence, such solutions cannot be considered as complete gravity duals of field theories, but they provide only approximate descriptions that may miss important long-distance details.

### D. Confining solutions

The solutions of this class are completely regular, and dual to confining, three-dimensional field theories. Here we present their IR expansions, discuss the gravitational invariants, and compute the Wilson loops. The expansion in proximity of the end of space  $\rho_o$ , is

$$\begin{aligned} \phi_C(\rho) &= \phi_I - \frac{(\rho - \rho_o)^2 e^{-2\sqrt{\frac{2}{3}} \phi_I} (e^{\sqrt{6} \phi_I} - 1)}{\sqrt{6}} \\ &+ \mathcal{O}((\rho - \rho_o)^4), \end{aligned} \quad (53)$$

$$\begin{aligned} \chi_C(\rho) &= \chi_I + \frac{\log(\rho - \rho_o)}{2} \\ &- \frac{1}{18} (\rho - \rho_o)^2 e^{-2\sqrt{\frac{2}{3}} \phi_I} (2e^{\sqrt{6} \phi_I} + 1) \\ &+ \mathcal{O}((\rho - \rho_o)^4), \end{aligned} \quad (54)$$

$$\begin{aligned}
 A_C(\rho) &= A_I + \frac{\log(\rho - \rho_o)}{2} \\
 &+ \frac{5}{18}(\rho - \rho_o)^2 e^{-2\sqrt{\frac{2}{3}}\phi_I} (2e^{\sqrt{6}\phi_I} + 1) \\
 &+ \mathcal{O}((\rho - \rho_o)^4). \tag{55}
 \end{aligned}$$

The gravity invariants in five dimensions are finite, and when restricted to the  $(\rho, \eta)$  plane, the metric reduces to

$$ds_2^2 = d\rho^2 + e^{4\chi_I}(\rho - \rho_o)^2 d\eta^2. \tag{56}$$

We fix  $\chi_I = 0$  in order to avoid a conical singularity. The integration constant  $A_I$  is trivial and can be reabsorbed by a rescaling of the three Minkowski directions. The constant  $\phi_I$  characterizes this one-parameter family of solutions. The curvature invariants of the lift to  $D = 10$  dimensions are regular, for all choices of  $0 \leq \theta \leq \pi/2$ .

In the study of the rectangular Wilson loop (in three dimensions) we fix  $\theta$ , and allow the two sides of the rectangle to align with time and one noncompact spacelike direction. The static potential  $E_W(L)$  is illustrated by Fig. 4, for two representative choices with  $\phi_o \pm 1$ . The short-distance Coulombic behavior gives way to the linear potential typical of confinement, and  $L$  is unbounded. For this reason, with some abuse of language, we call these

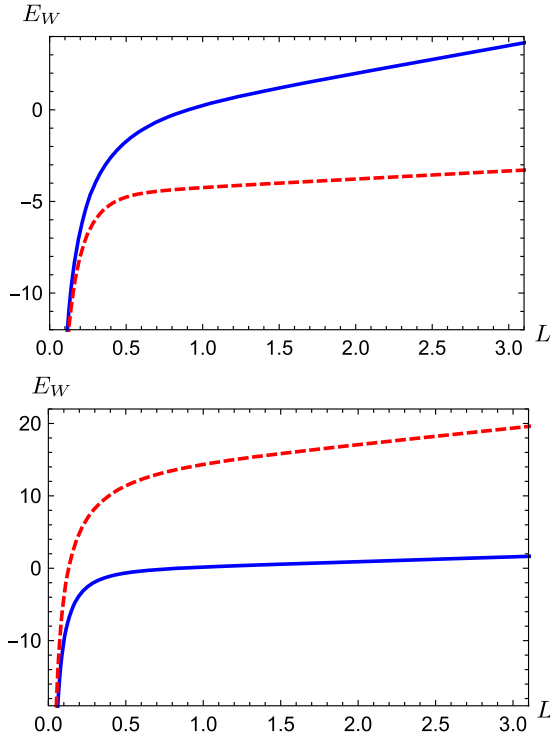


FIG. 4. Energy  $E_W$  as a function of the separation  $L$ , for two representative confining solutions, chosen to have  $A_I = 0 = \chi_I$ , and  $\phi_I = -1$  (top) or  $\phi_I = +1$  (bottom). Continuous (blue) lines correspond to configurations with  $\theta = 0$ , short-dashed (red) lines to configurations with  $\theta = \pi/2$ .

regular solutions *confining*. We can compute the string tension, and we find

$$\sigma_0 \equiv \lim_{\hat{\rho}_o \rightarrow \rho_o} F(\hat{\rho}_o, 0) = e^{2A_I - 2\chi_I - \sqrt{\frac{1}{6}}\phi_I}, \tag{57}$$

$$\sigma_{\pi/2} \equiv \lim_{\hat{\rho}_o \rightarrow \rho_o} F(\hat{\rho}_o, \pi/2) = e^{2A_I - 2\chi_I + 2\sqrt{\frac{1}{6}}\phi_I}. \tag{58}$$

The configuration with  $\theta = 0$  has lower energy in the case where  $\phi_I > 0$ , and vice versa.

#### IV. MASS SPECTRA AND PROBE APPROXIMATION

The spectrum of small fluctuations of a sigma model coupled to gravity of the form of Eqs. (2) and (13) in generic  $D$  dimensions can be interpreted in terms of the spectrum of bound states of the strongly-coupled dual field theory, by applying the dictionary of gauge-gravity dualities. We adopt the gauge-invariant formalism described in detail in Refs. [15–19]. Due to the divergences in the deep IR and far UV, we introduce two unphysical boundaries  $\rho_1 < \rho < \rho_2$  in the radial direction—the physical results are recovered in the limits  $\rho_2 \rightarrow +\infty$  and  $\rho_1 \rightarrow \rho_o$ . The calculation involves fluctuating solutions for which the metric has the DW form in  $D$  dimensions. The confining solutions assume the DW form in the dimensionally reduced ( $D = 4$ ) formulation of the theory. For the confining solutions, it is also understood that in the following equations (59)–(62) appearing in this section of the paper,  $\mathcal{A}$  is to be replaced by  $A$ .

The tensorial fluctuations  $e^\mu_\nu$  are gauge invariant, obey the equations of motion

$$[\partial_\rho^2 + (D-1)\partial_\rho \mathcal{A} \partial_\rho + e^{-2\mathcal{A}(\rho)} M^2] e^\mu_\nu = 0, \tag{59}$$

where  $M$  is the mass in  $D-1$  dimensions, and are subject to Neumann boundary conditions  $\partial_\rho e^\mu_\nu|_{\rho_i} = 0$ . The scalar gauge invariant fluctuations  $\mathbf{a}^a \equiv \varphi^a - \frac{\partial_\rho \Phi^a}{2(D-2)\partial_\rho \mathcal{A}} h$  are a combination of fluctuations  $\varphi^a$  of the scalar fields and  $h$  of the trace of the metric. They obey the following equations of motion and boundary conditions

$$\begin{aligned}
 0 &= [\mathcal{D}_\rho^2 + (D-1)\partial_\rho \mathcal{A} \mathcal{D}_\rho + e^{-2\mathcal{A}} M^2] \mathbf{a}^a \\
 &- \left[ V^a|_c + \frac{4(\partial_\rho \Phi^a V^b + V^a \partial_\rho \Phi^b) G_{bc}}{(D-2)\partial_\rho \mathcal{A}} \right. \\
 &\left. + \frac{16V \partial_\rho \Phi^a \partial_\rho \Phi^b G_{bc}}{(D-2)^2 (\partial_\rho \mathcal{A})^2} \right] \mathbf{a}^c, \tag{60}
 \end{aligned}$$

$$0 = \frac{2e^{2\mathcal{A}} \partial_\rho \Phi^a}{(D-2)M^2 \partial_\rho \mathcal{A}} \left[ \partial_\rho \Phi^b \mathcal{D}_\rho - \frac{4V \partial_\rho \Phi^b}{(D-2)\partial_\rho \mathcal{A}} - V^b \right] \mathbf{a}_b + \mathbf{a}^a \Big|_{\rho_i}. \tag{61}$$

The notation follows the conventions of Ref. [19]. The sigma-model metric being trivial, the covariant derivative simplifies to  $V^a|_c \equiv D_c V^a = \partial_c(G^{ab}\partial_b V)$ , and the background-covariant derivative to  $\mathcal{D}_\rho \mathbf{a}^a = \partial_\rho \mathbf{a}^a$ .

The *probe approximation* is defined according to the prescription tested in Ref. [131], and we use it as a diagnostic tool to identify particles coupled to the trace of the energy momentum tensor, because of their mixing with  $h$ . The probe approximation ignores the fluctuation  $h$ , in the definition of  $\mathbf{a}^a$ , yielding variables  $\mathbf{p}^a$  that satisfy

$$0 = [\mathcal{D}_\rho^2 + (D-1)\partial_\rho \mathcal{A} \mathcal{D}_\rho - e^{-2A} q^2] \mathbf{p}^a - V^a|_c \mathbf{p}^c, \quad (62)$$

subject to Dirichlet boundary conditions  $\mathbf{p}^a|_{\rho_i} = 0$ .

The fluctuation  $h$  is interpreted as the bulk field coupled to the dilatation operator in the dual field theory. If the approximation of ignoring  $h$  captures correctly the spectrum, then the associated scalar particle is not a dilaton. Conversely, the probe approximation either completely misses, or fails to capture the correct mass of, an approximate dilaton. We tested these ideas on a large selection of examples in Ref. [131].

In order to improve the convergence of the numerical computation of the spectrum, we make use of the UV expansions for the fluctuations given in Appendix B, setting up the boundary conditions such that only the subleading modes are retained. This is the customary prescription, as well as the one selected by the boundary conditions in Eq. (61), in the limit in which we remove the UV regulator (boundary) at  $\rho_2$ .

We start the analysis from the DW solutions. The result of the numerical study of the fluctuations for the  $(\phi_-, \mathcal{A}_-)$  solutions is displayed in Fig. 5, as a function of the parameter  $\phi_o$  characterizing this one-parameter family. We find it convenient to normalize the masses  $M$  of the spin-zero (blue disks) and spin-two states (red circles) so that the lightest tensor mode has unit mass.

For any finite value of  $\phi_o$  the spectrum is characterized by an unremarkable discrete sequence of states, and by the existence of a tachyon, which signals a fatal instability in the background solutions. Only in the strict limit  $\phi_o \rightarrow -\infty$  does the tachyon become exactly massless. In the same limit, the spectrum degenerates to a gapped continuum, in all the channels, for  $M^2 > 1$  (in units of the lightest tensor mode). This result reproduces the results quoted from the literature in Appendix A, for the  $n=2$  case, confirming that the gauge-invariant formalism we adopt, the choices of boundary conditions we impose, and the numerical strategy we deploy combine to correctly identify all the poles of the relevant two-point correlation functions.

By comparing the gauge-invariant spin-zero fluctuations to the probe approximation (the black diamonds in Fig. 5), we clearly see that the probe approximation fails most completely to capture the lightest (tachyonic) masses, for all values of  $\phi_o$ , so that we can establish that the dilaton

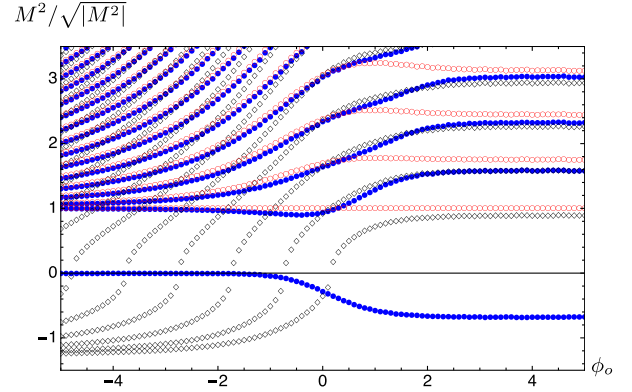


FIG. 5. Mass spectrum of the fluctuations of the negative DW solutions. The (red) circles are spin-two states, the (blue) disks are spin-zero states, and the (black) diamonds represent the probe approximation calculation of the same spin-zero masses. The masses  $M$  are normalized to the lightest spin-two state, and plotted as a function of  $\phi_o$ , defined in Eqs. (43) and (44). For  $\phi_o \rightarrow -\infty$  the backgrounds approach the supersymmetric solution in Eqs. (A3) and (A4)—or Eqs. (A7) and (A8). The numerical calculations are performed with finite cutoffs  $\rho_1 = 10^{-6}$  and  $\rho_2 = 8$ . We checked explicitly that these choices are close enough to the physical limits  $\rho_1 \rightarrow \rho_o = 0$  and  $\rho_2 \rightarrow +\infty$  that the numerical results do not display important residual spurious dependence on the cutoffs.

component is always important in such spin-zero objects. Mixing effects become prevalent for negative  $\phi_o$ . For large and positive values of  $\phi_o$ , the probe approximation captures well the excited scalar states, and hence yields a clear, unambiguous identification of the dilaton with the tachyon.

Fig. 6 displays the result of the study of the fluctuations for the DW solutions  $(\phi_+, \mathcal{A}_+)$ . These include the supersymmetric  $n=4$  case in Appendix A (marked for convenience by a vertical dashed line in the figure). The special limiting case of  $\phi_o \rightarrow +\infty$  is reached asymptotically at the right-hand side of the figure. The symbols (and colors) follow the same conventions as in Fig. 5.

One difference appears immediately evident; there is a region of parameter space, bounded by the supersymmetric  $n=4$  solution, for which  $\phi_o > -\frac{1}{2}\sqrt{\frac{3}{2}}\log(\frac{4}{3})$ , and in which all the scalar states have positive-definite mass squared. (We also saw in Sec. III C, and particularly in Sec. III C 1, that solutions of this type have a milder singularity.)

Once more the spectrum of the supersymmetric background is in agreement with the literature, which further confirms that our numerical strategy is reliable. The spectrum for  $\phi_o < -\frac{1}{2}\sqrt{\frac{3}{2}}\log(\frac{4}{3})$  always contains a tachyon, followed by a light scalar state and a densely packed sequence of heavy excitations. In the limit  $\phi_o \rightarrow -\infty$ , the spectrum agrees with the case of the supersymmetric solution  $(\phi_2, \mathcal{A}_2)$ , except for the addition of a tachyon. Indeed, this superficially surprising feature can be explained by close examination of the stream plot in

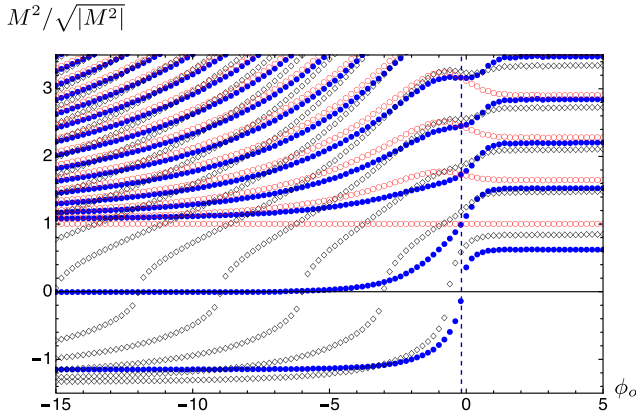


FIG. 6. Mass spectrum of the fluctuations of the positive DW solutions. The (red) circles are the spin-two states, the (blue) disks are the spin-zero states, and the (black) diamonds represent the probe approximation calculation of the spin-zero masses. The masses  $M$  are normalized to the lightest spin-two state, and plotted as a function of  $\phi_o$ , defined in Eqs. (46) and (47). The special case of the supersymmetric solutions in Eqs. (A5) and (A6) is the choice of  $\phi_o$  that yields a massless scalar state, and is marked by a vertical dashed line. The numerical calculations are performed with finite cutoffs  $\rho_1 = 10^{-6}$  and  $\rho_2 = 8$ . We checked explicitly that these choices are close enough to the physical limits  $\rho_1 \rightarrow \rho_o = 0$  and  $\rho_2 \rightarrow +\infty$  that the numerical results do not display any important residual spurious dependence on the cutoffs.

Fig. 2, from which one can see that it is possible to choose boundary conditions for the  $(\phi_+, \mathcal{A}_+)$  solutions that yield a trajectory approaching the special (supersymmetric) limit  $(\phi_2, \mathcal{A}_2)$  with  $\phi_o \rightarrow -\infty$ . Yet, eventually all the  $\phi_+(\rho)$  solutions turn positive (and divergent), close enough to the end of the space; the tachyon emerges as an unavoidable consequence of the intrinsic instability of these flows.

The comparison with the probe approximation is instructive; the tachyon is never captured by the probe approximation, which rather produces an arbitrary number of negative-mass-squared states, depending on  $\phi_o$ . Conversely, in the region of large and positive  $\phi_o$  the probe approximation highlights that an infinite number of scalars mix with the dilaton.

The spectrum of confining solutions with  $\phi = 0$  has been computed in Ref. [60], although only after truncating the tower of excitations of  $\phi$ . This background is sometimes called QCD<sub>3</sub> (with abuse of language) in the literature. In units of the lightest spin-two excitation the spectrum of mass of the tensors ( $T_3$  in Table 4 of Ref. [60]) is reported to be

$$M_2 = 1, 1.73, 2.44, .3.15, 3.86, 4.56, \dots \quad (63)$$

and for the scalars ( $S_3$  in Table 4 of Ref. [60])

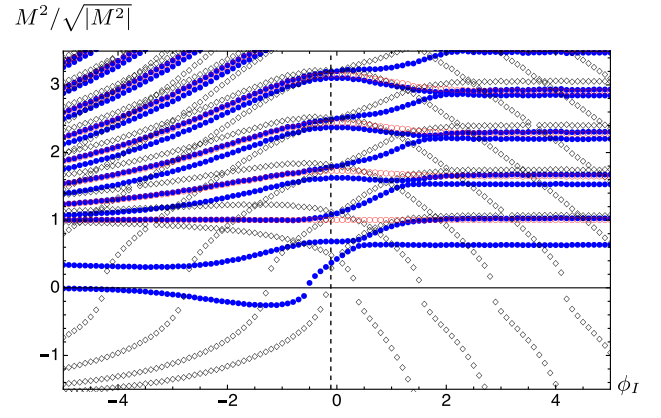


FIG. 7. Mass spectrum of the fluctuations of the confining solutions. The spectrum can be interpreted in terms of the masses of bound states in a confining theory in three dimensions. The (red) circles are the spin-two states, the (blue) disks are the spin-zero states, and the (black) diamonds represent the probe approximation calculation of the spin-zero masses. The masses  $M$  are normalized to the lightest spin-two state, and plotted as a function of  $\phi_I$ , defined in Eq. (53). The vertical dashed line denotes the value of the parameter  $\phi_I = \phi_I^* \simeq -0.067$  at which a phase transition takes place. The numerical calculations are performed with finite cutoffs  $\rho_1 = 10^{-6}$  and  $\rho_2 = 8$ . We checked explicitly that these choices are close enough to the physical limits  $\rho_1 \rightarrow \rho_o = 0$  and  $\rho_2 \rightarrow +\infty$  that the numerical results do not display any important residual spurious dependence on the cutoffs.

$$M_0 = 0.69, 1.62, 2.37, .3.10, 3.81, 4.53, \dots \quad (64)$$

We extend the numerical study to the whole one-parameter scion of solutions characterized by  $\phi_o$ , and retain both fluctuations of  $\phi$  and  $\chi$ . The resulting spectrum is displayed in Fig. 7. The masses of scalars (blue disks) and tensors (red circles) are plotted as a function of  $\phi_I$ . We also display the result of applying the probe approximation to the treatment of the scalars (black diamonds). For  $\phi_I = 0$ , the tensor masses, as well as the masses of half the scalars (the second, fourth, sixth, eighth, ...) are in excellent agreement with Ref. [60], confirming for the third time the robustness of our procedure. Yet, the truncation adopted in Ref. [60] misses the lightest of the scalar states, which can be decoupled only for  $\phi = 0$ —in this case, the probe approximation is accurate for the first, third, fifth, ..., scalar states, but only within a narrow range around  $\phi = 0$ .

The main feature that emerges is that the spectrum is positive definite only for  $\phi_I > \phi_I^* \simeq -0.52$ . For large and negative values of  $\phi_I$ , we find the emergence of a tachyon, signaling the appearance of an instability. The probe approximation fails to capture the features of the spectrum, even at the qualitative level, yielding an unphysical proliferation of tachyons.

In summary, in the case of the confining solutions, and for  $\phi_I > \phi_I^* \simeq -0.52$ , the solutions are regular (the curvature invariants computed in  $D = 5$  and  $D = 10$  dimensions

are all finite) and smooth (there is no conical singularity at the end of space), the spectrum is positive definite, and the calculation of the Wilson loop via the dual gravity prescription leads to the linear potential expected in a confining field theory (in three dimensions). All of these properties are preserved all the way along the scion of confining solutions until the critical value  $\phi_I^*$ , in proximity of which the lightest scalar separates from the rest of the spectrum, and becomes arbitrarily light, before turning into a tachyon. This light state, as shown by the probe approximation, has a substantial overlap with the dilaton, and couples to the trace of the energy-momentum tensor of the dual confining theory.

## V. FREE ENERGY AND STABILITY ANALYSIS

Because we regulate the theory by introducing two boundaries  $\rho_1$  and  $\rho_2$  in the radial direction of the geometry, the complete action in  $D = 5$  dimensions must include also boundary-localized terms,

$$\mathcal{S} = \mathcal{S}_5 + \sum_{i=1,2} (-)^i \int d^3x d\eta \sqrt{-\tilde{g}} \left[ \frac{K}{2} + \lambda_i \right] \Big|_{\rho_i}. \quad (65)$$

The Gibbons-Hawking-York (GHY) term is proportional to the extrinsic curvature  $K$ , and  $\lambda_i$  are boundary potentials. We choose  $\lambda_1 = -\partial_\rho A|_{\rho=\rho_1}$ , and, as in Ref. [12]—see also Eq. (3.66) of Ref. [153],

$$\lambda_2 = -\frac{3}{2} - \phi^2 \left( 1 + \frac{1}{\log(k^2 z_2^2)} \right), \quad (66)$$

where  $z_2 \equiv e^{-\rho_2}$ , and the freedom in the choice of  $k$  reflects the scheme-dependence of the result.

The explicit appearance of the term containing the unphysical constant  $k$  in this result is a peculiarity of this model, distinguishing it from those in Refs. [1,2]. It is due to the mass of the scalar field corresponding to the deforming field theory operator exactly saturating the BF unitarity bound. In this sense, this model is a more direct realization of the ideas exposed in Ref. [3], where the proximity to the BF bound is the starting point of the analysis. As we shall see shortly, though, our results here are qualitatively similar to those in Refs. [1,2].

The need for counterterms that are quadratic in  $\phi$ , and their scheme dependence, imply that the concavity theorems do not hold for the free energy of this system. The free energy  $F$  and its density  $\mathcal{F}$  are defined as

$$F \equiv - \lim_{\rho_1 \rightarrow \rho_0} \lim_{\rho_2 \rightarrow +\infty} \mathcal{S}^{\text{on-shell}} \equiv \int d^3x d\eta \mathcal{F}, \quad (67)$$

and by using the equations of motion, supplemented by the observation that Eq. (20) defines a conserved quantity along the radial direction  $\rho$ , we find

$$\mathcal{F} = - \lim_{\rho_2 \rightarrow +\infty} e^{3A-\chi} (\partial_\rho A + \lambda_2) \Big|_{\rho_2}. \quad (68)$$

We can now use the UV expansions, take the  $e^{-\rho_2} \rightarrow 0$  limit, and arrive at

$$\mathcal{F} = \frac{1}{18} e^{3A_U - \chi_U} (2\phi_2^2 + 9\phi_2\phi_{2l} - 2\phi_{2l}^2 + 24\chi_4 - 9\phi_{2l}^2 \log(k)). \quad (69)$$

For the DW solutions, further simplifications yield

$$\mathcal{F}^{(DW)} = \frac{1}{8} e^{\frac{3}{2}A_U} (4\phi_2 - \phi_{2l} - 4\phi_{2l} \log(k)) \phi_{2l}. \quad (70)$$

Along the lines of Ref. [1], we find it convenient to define a scale  $\Lambda$  as follows [162]:

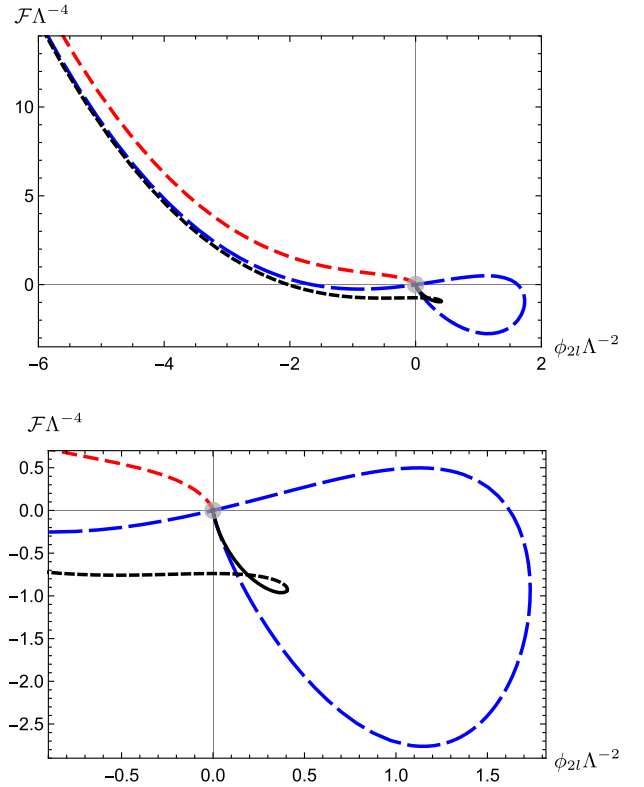


FIG. 8. The free energy density  $\mathcal{F}\Lambda^{-4}$ , defined in Eq. (70), expressed in units of the scale-setting parameter  $\Lambda$  defined in Eq. (71), plotted as a function of the deformation parameter  $\phi_{2l}\Lambda^{-2}$ , for the various classes of solutions considered in the paper. For the confining solutions, the tachyonic backgrounds are denoted by continuous (black) lines, while backgrounds with a positive-definite mass spectrum are represented by the (black) short-dashed line. The long-dashed (blue) lines are the positive DW solutions, the dashed (red) lines are the negative DW solutions, while the gray disk represents the supersymmetric solutions. The bottom panel is a detail of the top one.

$$\Lambda^{-1} \equiv \int_{\rho_o}^{\infty} d\rho e^{\chi(\rho)-A(\rho)}. \quad (71)$$

While this is not a unique choice, its simplicity and universality gives it a practical value for our applications. In the calculation of the free energy density, we set  $k = \Lambda$ , as this quantity scales with dilatations in the same way as  $z^{-1}$ .

We display in Fig. 8 the result of the calculation of  $\mathcal{F}\Lambda^{-4}$  as a function of the source  $\phi_{2l}\Lambda^{-2}$ , for the three classes of negative DW, positive DW and confining solutions. For negative values of  $\phi_{2l}\Lambda^{-2}$ , as we saw the regular confining solutions have a positive definite spectrum (as  $\phi_l > \phi_l^*$ ), and furthermore their free energy is the lowest among the solutions we considered. When  $\phi_{2l}\Lambda^{-2}$  is positive, but small, we still find regular confining solutions, but the lightest scalar state has lower mass, which vanishes when  $\phi_l = \phi_l^* \simeq -0.52$ , after which it turns tachyonic. There is hence a regime of parameter space in which the lightest scalar has suppressed mass. But these solutions are metastable; the positive DW solutions (despite being singular) have lower free energy when  $\phi_{2l}\Lambda^{-2} > \phi_{2l}^*\Lambda^{-2} \simeq 0.13$ , the critical value identified by the crossing in Fig. 8 (corresponding to  $\phi_l^* \simeq -0.067$ ). Once more, as in the models in Refs. [1,2], we find that the lightest scalar can be identified with a parametrically light dilaton along the metastable solutions. In the stable solutions the lightest scalar is still an approximate dilaton, but not parametrically light.

## VI. CONCLUSION AND OUTLOOK

We studied new classes of background solutions of maximal supergravity in  $D = 5$  dimensions, truncated to retain only one scalar field. This is the theory related to the dual of the Coulomb branch of  $\mathcal{N} = 4$  SYM. We focused on solutions that are regular, have a positive definite spectrum, and can be interpreted as the gravity dual of confining field theories in three dimensions. We found evidence that the lightest scalar state is an approximate dilaton, and can be made parametrically light, in a region of parameter space in which these new regular solutions are metastable.

The study confirms, in a lower-dimensional simple setting, for a well known example of gauge-gravity duality related to the study of  $\mathcal{N} = 4$  SYM, the qualitative features that emerged in the models in Refs. [1,2]. We notice the emergence of a first-order phase transition separating the metastable from the stable portions of the parameter space of the new confining solutions. As in Refs. [4–6], the approximate dilaton is not parametrically light in the stable solutions, confirming this generic feature also in confining theories in three dimensions.

Further exploration of the catalog of supergravity theories will possibly help to understand whether the aforementioned results are universal or model dependent. Of particular interest would be to ascertain whether it is possible—and under what conditions—to find systems

for which the phase transition is weak enough to render the dilaton parametrically light already in the stable region of parameter space, in proximity of the phase transition itself. It would also be interesting to see whether systems exist for which the phase transition is of second order.

## ACKNOWLEDGMENTS

M. P. would like to thank Carlos Nunez for a useful discussion. The work of M. P. has been supported in part by the STFC Consolidated Grants No. ST/P00055X/1 and No. ST/T000813/1. M. P. has also received funding from the European Research Council (ERC) under the European Union Horizon 2020 research and innovation programme under Grant Agreement No. 813942. J. R. is supported by STFC, through the studentship No. ST/R505158/1.

## APPENDIX A: THE TWO SUPERSYMMETRIC SOLUTIONS

The first-order Eqs. (8) can be solved exactly by changing variable according to  $\partial_\rho = e^{\frac{\phi}{\sqrt{6}}}\partial_\tau$ . The first-order equations are then

$$\partial_\tau \phi(\tau) = -\frac{4}{\sqrt{6}} \sinh\left(\sqrt{\frac{3}{2}}\phi(\tau)\right), \quad (A1)$$

$$\begin{aligned} \partial_\tau \mathcal{A}(\tau) &= \cosh\left(\sqrt{\frac{3}{2}}\phi(\tau)\right) \\ &\quad - \frac{1}{3} \sinh\left(\sqrt{\frac{3}{2}}\phi(\tau)\right). \end{aligned} \quad (A2)$$

There are two exact solutions [23,147,151]. The case of  $n = 2$  is given by

$$\phi_2(\tau) = -\frac{4}{\sqrt{6}} \operatorname{arctanh}(e^{-2(\tau-\tau_o)}), \quad (A3)$$

$$\begin{aligned} \mathcal{A}_2(\tau) &= \mathcal{A}_o + \tau - \tau_o - \frac{1}{3} \operatorname{arctanh}(e^{-2(\tau-\tau_o)}) \\ &\quad + \frac{1}{2} \log(1 - e^{-4(\tau-\tau_o)}), \end{aligned} \quad (A4)$$

and the  $n = 4$  case by

$$\phi_4(\tau) = \frac{4}{\sqrt{6}} \operatorname{arctanh}(e^{-2(\tau-\tau_o)}), \quad (A5)$$

$$\begin{aligned} \mathcal{A}_4(\tau) &= \mathcal{A}_o + \tau - \tau_o + \frac{1}{3} \operatorname{arctanh}(e^{-2(\tau-\tau_o)}) \\ &\quad + \frac{1}{2} \log(1 - e^{-4(\tau-\tau_o)}), \end{aligned} \quad (A6)$$

where  $\tau_o$  and  $\mathcal{A}_o$  are two integration constants.

The two classes of supersymmetric solutions can be rewritten as expansions valid for  $0 < \rho - \rho_o \ll 1$ ,

$$\begin{aligned} \phi_2(\rho) &= -\sqrt{\frac{3}{8}} \log\left(\frac{9}{4}\right) + \sqrt{\frac{3}{2}} \log(\rho - \rho_o) \\ &\quad - \sqrt{\frac{2}{243}} (\rho - \rho_o)^3 + \frac{17}{1701} \sqrt{\frac{2}{3}} (\rho - \rho_o)^6 + \dots, \end{aligned} \quad (\text{A7})$$

$$\begin{aligned} \mathcal{A}_2(\rho) &= \mathcal{A}_I + \log(\rho - \rho_o) + \frac{2}{27} (\rho - \rho_o)^3 \\ &\quad - \frac{22}{5103} (\rho - \rho_o)^6 + \dots. \end{aligned} \quad (\text{A8})$$

and

$$\begin{aligned} \phi_4(\rho) &= -\frac{1}{2} \sqrt{\frac{3}{2}} \log\left(\frac{4}{3}\right) - \frac{1}{2} \sqrt{\frac{3}{2}} \log(\rho - \rho_o) \\ &\quad + \frac{4}{15} \sqrt{2} (\rho - \rho_o)^{3/2} - \frac{28}{225} \sqrt{\frac{2}{3}} (\rho - \rho_o)^3 + \dots, \end{aligned} \quad (\text{A9})$$

$$\begin{aligned} \mathcal{A}_4(\rho) &= \mathcal{A}_I + \frac{1}{4} \log(\rho - \rho_o) + \frac{16}{15\sqrt{3}} (\rho - \rho_o)^{3/2} \\ &\quad - \frac{52}{675} (\rho - \rho_o)^3 + \dots. \end{aligned} \quad (\text{A10})$$

The  $n = 2$  case is the limit  $\phi_o \rightarrow -\infty$  of the general DW solutions in Eqs. (43) and (44), while the  $n = 4$  case is recovered with the choice  $\phi_o = -\frac{1}{2} \sqrt{\frac{3}{2}} \log\left(\frac{4}{3}\right)$  in Eqs. (46) and (47).

Both solutions exhibit a naked singularity in  $D = 5$  dimensions, which softens in  $D = 10$  dimensions. For the  $n = 2$  solutions  $(\phi_2, \mathcal{A}_2)$  we find

$$\mathcal{R}_{10, \hat{M}\hat{N}} \mathcal{R}_{10}^{\hat{M}\hat{N}} = \frac{135}{4 \cos^2(\theta) (\rho - \rho_o)^3} + \dots. \quad (\text{A11})$$

For the ( $n = 4$ ) solutions given by  $(\phi_4, \mathcal{A}_4)$  the behavior of this invariant is milder,

$$\mathcal{R}_{10, \hat{M}\hat{N}} \mathcal{R}_{10}^{\hat{M}\hat{N}} = \frac{5 \sin^4(2\theta)}{8 \sin^{10}(\theta)} + \dots. \quad (\text{A12})$$

The singularity at the equator of  $S^5$  displayed by the curvature invariant in Eqs. (A11) and (A12) at the end of space signals the incompleteness of the supergravity description in both supersymmetric cases.

The Wilson loops for the supersymmetric solutions have been computed in Ref. [23]. We display our result in Fig. 9 as a test of our procedure. In the case of the  $n = 2$  solutions  $(\phi_2, \mathcal{A}_2)$ , for both  $\theta = 0, \pi/2$  we find a monotonic potential, and a maximum value of  $L = L_{\max}$ . In the case  $n = 4$  of  $(\phi_4, \mathcal{A}_4)$ , there is a very major difference between the two cases with  $\theta = 0, \pi/2$ . The case of  $\theta = 0$  displays

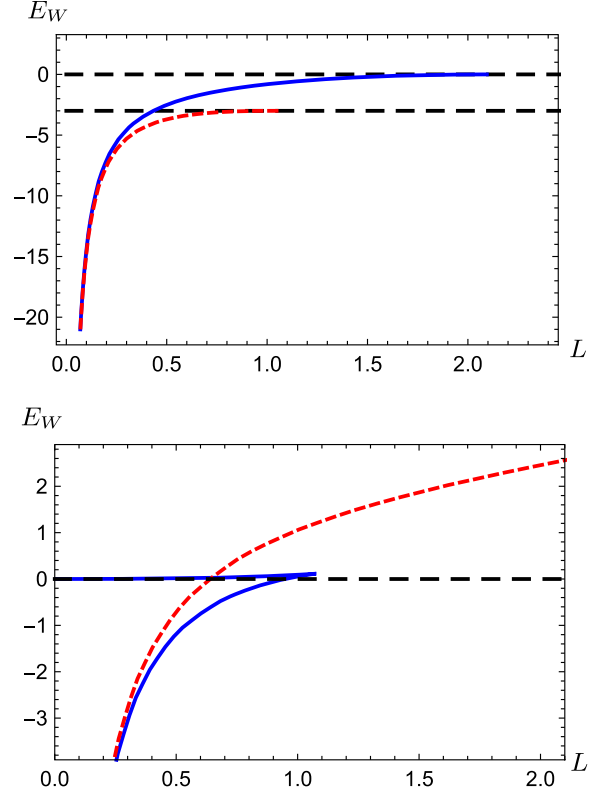


FIG. 9. Energy  $E_W$  as a function of the separation  $L$ , for supersymmetric solutions  $n = 2$ ,  $(\phi_2, \mathcal{A}_2)$  (top) and  $n = 4$ ,  $(\phi_4, \mathcal{A}_4)$  (bottom), and chosen to have  $\mathcal{A}_I = 0$ . Continuous (blue) lines correspond to configurations with  $\theta = 0$ , short-dashed (red) lines depict configurations with  $\theta = \pi/2$ , and long-dashed (black) lines represent configurations reaching exactly the end of space.

the features expected by a first order phase transition, with long-distance screening. Conversely, for  $\theta = \pi/2$  we find a linear potential at asymptotically large  $L$ , which is unbounded; this configuration has higher energy than the  $\theta = 0$  one.

For the  $n = 2$  solutions  $(\phi_2, \mathcal{A}_2)$  in Eqs. (A3) and (A4), the two-point function of the operator  $\mathcal{O}$  dual to the scalar  $\phi$  can be found in Sec. 3.3 of Ref. [153] (see also Eq. (8.6) of Ref. [12]);

$$\langle \mathcal{O}(q) \mathcal{O}(-q) \rangle = \frac{16}{3q^2} - 4(\psi(a(q) + 1) - \psi(1)), \quad (\text{A13})$$

and for the tensors

$$\langle T_{\mu\nu} T_{\rho\sigma} \rangle \propto \frac{q^2}{2\kappa'} \left[ \frac{1}{3} - \frac{q^2}{2} (\psi(a(q) + 1) - \psi(1)) \right], \quad (\text{A14})$$

where  $\psi$  is the digamma function,  $q$  the four-momentum in Euclidean signature,  $\kappa'$  is a constant, and  $a$  is

$$a(q) \equiv -\frac{1}{2} + \frac{1}{2} \sqrt{1+q^2}. \quad (\text{A15})$$

The scalar correlator displays a massless pole, a gap and a continuum cut; the tensor differs by the absence of the massless state.

The  $n = 4$  solutions  $(\phi_4, \mathcal{A}_4)$  in Eqs. (A5) and (A6), have a discrete spectrum, for example described in Eq. (26) of Ref. [147]. With  $j = 0, 1, \dots$ , the spectrum is given by  $M \propto \sqrt{j(j+1)/2} \simeq 0, 1, 1.7, 2.5, 3.2, \dots$ . The spectrum of tensors can be found for example in Eq. (45) of Ref. [151], according to which it agrees with that of the scalars ‘... to an extremely good approximation ...’, but for the fact that there is no zero mode.

The results of studying the Wilson loops agree with Figs. 1, 4, and 5, of Ref. [23]. We relied on numerical solutions guided by the asymptotic IR expansions, rather than using the exact solutions as in Ref. [23]. Our numerical study of the spectrum yields numerical results in splendid agreement with pre-existing calculations, as can be seen in Figs. 5 and 6. These results and their agreement with earlier studies of the supersymmetric solutions confirm the robustness of our formalism and numerical strategy.

## APPENDIX B: EXPANSIONS FOR THE FLUCTUATIONS

In the numerical calculation of the spectra, we used the asymptotic expansions of the gauge-invariant fluctuations, as a way to optimize the decoupling of spurious cutoff effects present at finite  $\rho_2$ . In the case of DW solutions, we find that we can expand the physical fluctuations as follows:

$$\mathbf{a}^\phi = \mathbf{a}_{2l}^\phi \log(z)z^2 + \mathbf{a}_2^\phi z^2 + \mathcal{O}(z^4), \quad (\text{B1})$$

$$\begin{aligned} \mathbf{e}_\nu^\mu &= (\mathbf{e}_0)_\nu^\mu \left( 1 - \frac{e^{-8A_U}}{4} q^2 z^2 - \frac{e^{-16A_U}}{16} q^4 \log(z)z^4 \right) \\ &+ (\mathbf{e}_4)_\nu^\mu z^4 + \mathcal{O}(z^6), \end{aligned} \quad (\text{B2})$$

In these expressions,  $\mathbf{a}_{2l}^\phi$ ,  $\mathbf{a}_2^\phi$ ,  $(\mathbf{e}_0)_\nu^\mu$ , and  $(\mathbf{e}_4)_\nu^\mu$  are the integration constants governing the solutions of the second-order linearized equations, half of which are determined by the boundary conditions. In the probe approximation, the expansion for the scalars  $\mathbf{p}^\phi$  is of the same form, up to  $\mathcal{O}(z^4)$ ,

$$\mathbf{p}^\phi = \mathbf{p}_{2l}^\phi \log(z)z^2 + \mathbf{p}_2^\phi z^2 + \mathcal{O}(z^4). \quad (\text{B3})$$

The confining solutions do not satisfy the DW conditions. For the scalars we find

$$\mathbf{a}^\phi = \mathbf{a}_{2l}^\phi \log(z)z^2 + \mathbf{a}_2^\phi z^2 + \mathcal{O}(z^4), \quad (\text{B4})$$

$$\begin{aligned} \mathbf{a}^\chi &= \mathbf{a}_0^\chi \left( 1 - \frac{e^{-2A_U+2\chi_U}}{4} q^2 z^2 + \right. \\ &\left. - \frac{e^{-4A_U+4\chi_U}}{16} q^4 \log(z)z^4 \right) + \mathbf{a}_4^\chi z^4 + \mathcal{O}(z^6), \end{aligned} \quad (\text{B5})$$

where  $\mathbf{a}_{2l}^\phi$ ,  $\mathbf{a}_2^\phi$ ,  $\mathbf{a}_0^\chi$ , and  $\mathbf{a}_4^\chi$  are the free parameters. For the probe approximation of the scalars, the free parameters are  $\mathbf{p}_{2l}^\phi$ ,  $\mathbf{p}_2^\phi$ ,  $\mathbf{p}_0^\chi$ , and  $\mathbf{p}_4^\chi$ , and as a result of mixing in the second derivative of the potential in Eq. (62) we have

$$\mathbf{p}^\phi = \mathbf{p}_{2l}^\phi \log(z)z^2 + \mathbf{p}_2^\phi z^2 + \mathcal{O}(z^4), \quad (\text{B6})$$

$$\mathbf{p}^\chi = \mathbf{p}_{2l}^\chi \log(z)z^2 + \mathbf{p}_2^\chi z^2 + \mathcal{O}(z^4). \quad (\text{B7})$$

For the tensor fluctuations we find

$$\begin{aligned} \mathbf{e}_\nu^\mu &= (\mathbf{e}_0)_\nu^\mu \left( 1 - \frac{1}{4} e^{-2A_U+2\chi_U} q^2 z^2 \right. \\ &\left. - \frac{1}{16} e^{-4A_U+4\chi_U} q^4 \log(z)z^4 \right) + (\mathbf{e}_4)_\nu^\mu z^4 + \mathcal{O}(z^6). \end{aligned} \quad (\text{B8})$$

- 
- [1] D. Elander, M. Piai, and J. Roughley, Dilatonic states near holographic phase transitions, *Phys. Rev. D* **103**, 106018 (2021).
- [2] D. Elander, M. Piai, and J. Roughley, Light dilaton in a metastable vacuum, *Phys. Rev. D* **103**, 046009 (2021).
- [3] D. B. Kaplan, J. W. Lee, D. T. Son, and M. A. Stephanov, Conformality lost, *Phys. Rev. D* **80**, 125005 (2009).
- [4] V. Gorbenko, S. Rychkov, and B. Zan, Walking, weak first-order transitions, and complex CFTs, *J. High Energy Phys.* **10** (2018) 108.
- [5] V. Gorbenko, S. Rychkov, and B. Zan, Walking, weak first-order transitions, and complex CFTs II. Two-dimensional Potts model at  $Q > 4$ , *SciPost Phys.* **5**, 050 (2018).
- [6] A. Pomarol, O. Pujolas, and L. Salas, Holographic conformal transition and light scalars, *J. High Energy Phys.* **10** (2019) 202.
- [7] P. Breitenlohner and D. Z. Freedman, Stability in gauged extended supergravity, *Ann. Phys. (N.Y.)* **144**, 249 (1982).

- [8] J. M. Maldacena, The large  $N$  limit of superconformal field theories and supergravity, *Int. J. Theor. Phys.* **38**, 1113 (1999); *Adv. Theor. Math. Phys.* **2**, 231 (1998).
- [9] S. S. Gubser, I. R. Klebanov, and A. M. Polyakov, Gauge theory correlators from noncritical string theory, *Phys. Lett. B* **428**, 105 (1998).
- [10] E. Witten, Anti-de Sitter space and holography, *Adv. Theor. Math. Phys.* **2**, 253 (1998).
- [11] O. Aharony, S. S. Gubser, J. M. Maldacena, H. Ooguri, and Y. Oz, Large  $N$  field theories, string theory and gravity, *Phys. Rep.* **323**, 183 (2000).
- [12] M. Bianchi, D. Z. Freedman, and K. Skenderis, Holographic renormalization, *Nucl. Phys.* **B631**, 159 (2002).
- [13] K. Skenderis, Lecture notes on holographic renormalization, *Classical Quant. Grav.* **19**, 5849 (2002).
- [14] I. Papadimitriou and K. Skenderis, AdS/CFT correspondence and geometry, *IRMA Lect. Math. Theor. Phys.* **8**, 73 (2005).
- [15] M. Bianchi, M. Prisco, and W. Mueck, New results on holographic three point functions, *J. High Energy Phys.* **11** (2003) 052.
- [16] M. Berg, M. Haack, and W. Mueck, Bulk dynamics in confining gauge theories, *Nucl. Phys.* **B736**, 82 (2006).
- [17] M. Berg, M. Haack, and W. Mueck, Glueballs vs gluino-balls: Fluctuation spectra in non-AdS/non-CFT, *Nucl. Phys.* **B789**, 1 (2008).
- [18] D. Elander, Glueball spectra of SQCD-like theories, *J. High Energy Phys.* **03** (2010) 114.
- [19] D. Elander and M. Piai, Light scalars from a compact fifth dimension, *J. High Energy Phys.* **01** (2011) 026.
- [20] S. J. Rey and J. T. Yee, Macroscopic strings as heavy quarks in large  $N$  gauge theory and anti-de Sitter supergravity, *Eur. Phys. J. C* **22**, 379 (2001).
- [21] J. M. Maldacena, Wilson Loops in Large  $N$  Field Theories, *Phys. Rev. Lett.* **80**, 4859 (1998).
- [22] Y. Kinar, E. Schreiber, and J. Sonnenschein, Q anti-Q potential from strings in curved space-time: Classical results, *Nucl. Phys.* **B566**, 103 (2000).
- [23] A. Brandhuber and K. Sfetsos, Wilson loops from multicenter and rotating branes, mass gaps and phase structure in gauge theories, *Adv. Theor. Math. Phys.* **3**, 851 (1999).
- [24] S. D. Avramis, K. Sfetsos, and K. Siampos, Stability of strings dual to flux tubes between static quarks in  $N = 4$  SYM, *Nucl. Phys.* **B769**, 44 (2007).
- [25] C. Nunez, M. Piai, and A. Rago, Wilson loops in string duals of walking and flavored systems, *Phys. Rev. D* **81**, 086001 (2010).
- [26] A. F. Faedo, M. Piai, and D. Schofield, On the stability of multiscale models of dynamical symmetry breaking from holography, *Nucl. Phys.* **B880**, 504 (2014).
- [27] S. S. Gubser, Curvature singularities: The good, the bad, and the naked, *Adv. Theor. Math. Phys.* **4**, 679 (2000).
- [28] L. J. Romans, The  $F(4)$  gauged supergravity in six-dimensions, *Nucl. Phys.* **B269**, 691 (1986).
- [29] L. J. Romans, Massive  $N = 2a$  supergravity in ten-dimensions, *Phys. Lett.* **169B**, 374 (1986).
- [30] A. Brandhuber and Y. Oz, The D-4—D-8 brane system and five-dimensional fixed points, *Phys. Lett. B* **460**, 307 (1999).
- [31] M. Cvetič, H. Lu, and C. N. Pope, Gauged Six-Dimensional Supergravity from Massive Type IIA, *Phys. Rev. Lett.* **83**, 5226 (1999).
- [32] J. Hong, J. T. Liu, and D. R. Mayerson, Gauged six-dimensional supergravity from warped IIB reductions, *J. High Energy Phys.* **09** (2018) 140.
- [33] J. Jeong, O. Kelekci, and E. O. Colgain, An alternative IIB embedding of  $F(4)$  gauged supergravity, *J. High Energy Phys.* **05** (2013) 079.
- [34] R. D’Auria, S. Ferrara, and S. Vaula, Matter coupled  $F(4)$  supergravity and the AdS(6) / CFT(5) correspondence, *J. High Energy Phys.* **10** (2000) 013.
- [35] L. Andrianopoli, R. D’Auria, and S. Vaula, Matter coupled  $F(4)$  gauged supergravity Lagrangian, *J. High Energy Phys.* **05** (2001) 065.
- [36] M. Nishimura, Conformal supergravity from the AdS/CFT correspondence, *Nucl. Phys.* **B588**, 471 (2000).
- [37] S. Ferrara, A. Kehagias, H. Partouche, and A. Zaffaroni, AdS(6) interpretation of 5-D superconformal field theories, *Phys. Lett. B* **431**, 57 (1998).
- [38] U. Gursoy, C. Nunez, and M. Schwelling, RG flows from spin(7), CY 4 fold and HK manifolds to AdS, Penrose limits and pp waves, *J. High Energy Phys.* **06** (2002) 015.
- [39] C. Nunez, I. Y. Park, M. Schwelling, and T. A. Tran, Supergravity duals of gauge theories from  $F(4)$  gauged supergravity in six-dimensions, *J. High Energy Phys.* **04** (2001) 025.
- [40] P. Karndumri, Holographic RG flows in six dimensional  $F(4)$  gauged supergravity, *J. High Energy Phys.* **01** (2013) 134; Erratum, *J. High Energy Phys.* **06** (2015) 165.
- [41] Y. Lozano, E. O. Colgain, D. Rodriguez-Gomez, and K. Sfetsos, Supersymmetric AdS<sub>6</sub> via T Duality, *Phys. Rev. Lett.* **110**, 231601 (2013).
- [42] P. Karndumri, Gravity duals of 5D  $N = 2$  SYM theory from  $F(4)$  gauged supergravity, *Phys. Rev. D* **90**, 086009 (2014).
- [43] C. M. Chang, M. Fluder, Y. H. Lin, and Y. Wang, Romans supergravity from five-dimensional holograms, *J. High Energy Phys.* **05** (2018) 039.
- [44] M. Gutperle, J. Kaidi, and H. Raj, Mass deformations of 5d SCFTs via holography, *J. High Energy Phys.* **02** (2018) 165.
- [45] N. Kim and M. Shim, Wrapped brane solutions in romans  $F(4)$  gauged supergravity, *Nucl. Phys.* **B951**, 114882 (2020).
- [46] K. Chen and M. Gutperle, Holographic line defects in  $F(4)$  gauged supergravity, *Phys. Rev. D* **100**, 126015 (2019).
- [47] C. Hoyos, N. Jokela, and D. Logares, Scattering length in holographic confining theories, *Phys. Rev. D* **102**, 086006 (2020).
- [48] M. Suh, Supersymmetric AdS<sub>6</sub> black holes from  $F(4)$  gauged supergravity, *J. High Energy Phys.* **01** (2019) 035.
- [49] M. Suh, Supersymmetric AdS<sub>6</sub> black holes from matter coupled  $F(4)$  gauged supergravity, *J. High Energy Phys.* **02** (2019) 108.
- [50] C. K. Wen and H. X. Yang, QCD(4) glueball masses from AdS(6) black hole description, *Mod. Phys. Lett. A* **20**, 997 (2005).
- [51] S. Kuperstein and J. Sonnenschein, Non-critical, near extremal AdS(6) background as a holographic laboratory

- of four dimensional YM theory, *J. High Energy Phys.* **11** (2004) 026.
- [52] D. Elander, A. F. Faedo, C. Hoyos, D. Mateos, and M. Piai, Multiscale confining dynamics from holographic RG flows, *J. High Energy Phys.* **05** (2014) 003.
- [53] D. Elander, M. Piai, and J. Roughley, Holographic glueballs from the circle reduction of Romans supergravity, *J. High Energy Phys.* **02** (2019) 101.
- [54] H. Nastase, D. Vaman, and P. van Nieuwenhuizen, Consistent nonlinear K K reduction of 11-d supergravity on AdS(7) x S(4) and selfduality in odd dimensions, *Phys. Lett. B* **469**, 96 (1999).
- [55] M. Pernici, K. Pilch, and P. van Nieuwenhuizen, Gauged maximally extended supergravity in seven-dimensions, *Phys. Lett.* **143B**, 103 (1984).
- [56] M. Pernici, K. Pilch, P. van Nieuwenhuizen, and N. P. Warner, Noncompact gaugings and critical points of maximal supergravity in seven-dimensions, *Nucl. Phys.* **B249**, 381 (1985).
- [57] H. Lu and C. N. Pope, Exact embedding of  $N = 1, D = 7$  gauged supergravity in  $D = 11$ , *Phys. Lett. B* **467**, 67 (1999).
- [58] V. L. Campos, G. Ferretti, H. Larsson, D. Martelli, and B. E. W. Nilsson, A study of holographic renormalization group flows in  $D = 6$  and  $D = 3$ , *J. High Energy Phys.* **06** (2000) 023.
- [59] E. Witten, Anti-de Sitter space, thermal phase transition, and confinement in gauge theories, *Adv. Theor. Math. Phys.* **2**, 505 (1998).
- [60] R. C. Brower, S. D. Mathur, and C. I. Tan, Glueball spectrum for QCD from AdS supergravity duality, *Nucl. Phys.* **B587**, 249 (2000).
- [61] S. Matsuzaki and K. Yamawaki, Dilaton Chiral Perturbation Theory: Determining the Mass and Decay Constant of the Technidilaton on the Lattice, *Phys. Rev. Lett.* **113**, 082002 (2014).
- [62] M. Golterman and Y. Shamir, Low-energy effective action for pions and a dilatonic meson, *Phys. Rev. D* **94**, 054502 (2016).
- [63] A. Kasai, K. I. Okumura, and H. Suzuki, A dilaton-pion mass relation, [arXiv:1609.02264](https://arxiv.org/abs/1609.02264).
- [64] M. Golterman and Y. Shamir, Effective action for pions and a dilatonic meson, *Proc. Sci., LATTICE2016* (2016) 205.
- [65] M. Hansen, K. Langaebler, and F. Sannino, Extending chiral perturbation theory with an isosinglet scalar, *Phys. Rev. D* **95**, 036005 (2017).
- [66] M. Golterman and Y. Shamir, Effective pion mass term and the trace anomaly, *Phys. Rev. D* **95**, 016003 (2017).
- [67] T. Appelquist, J. Ingoldby, and M. Piai, Dilaton EFT framework for lattice data, *J. High Energy Phys.* **07** (2017) 035.
- [68] T. Appelquist, J. Ingoldby, and M. Piai, Analysis of a dilaton EFT for lattice data, *J. High Energy Phys.* **03** (2018) 039.
- [69] M. Golterman and Y. Shamir, Large-mass regime of the dilaton-pion low-energy effective theory, *Phys. Rev. D* **98**, 056025 (2018).
- [70] O. Cata and C. Muller, Chiral effective theories with a light scalar at one loop, *Nucl. Phys.* **B952**, 114938 (2020).
- [71] T. Appelquist, J. Ingoldby, and M. Piai, Dilaton potential and lattice data, *Phys. Rev. D* **101**, 075025 (2020).
- [72] O. Catà, R. J. Crewther, and L. C. Tunstall, Crawling technicolor, *Phys. Rev. D* **100**, 095007 (2019).
- [73] T. V. Brown, M. Golterman, S. Krojer, Y. Shamir, and K. Splittorff, The  $\epsilon$ -regime of dilaton chiral perturbation theory, *Phys. Rev. D* **100**, 114515 (2019).
- [74] S. Coleman, *Aspects of Symmetry: Selected Erice Lectures* (Cambridge University Press, Cambridge, England, 2010).
- [75] A. A. Migdal and M. A. Shifman, Dilaton effective lagrangian in gluodynamics, *Phys. Lett.* **114B**, 445 (1982).
- [76] C. N. Leung, S. T. Love, and W. A. Bardeen, Spontaneous symmetry breaking in scale invariant quantum electrodynamics, *Nucl. Phys.* **B273**, 649 (1986).
- [77] W. A. Bardeen, C. N. Leung, and S. T. Love, The Dilaton and Chiral Symmetry Breaking, *Phys. Rev. Lett.* **56**, 1230 (1986).
- [78] K. Yamawaki, M. Bando, and K. I. Matumoto, Scale Invariant Technicolor Model and a Technidilaton, *Phys. Rev. Lett.* **56**, 1335 (1986).
- [79] Y. Aoki *et al.* (LatKMI Collaboration), Light composite scalar in eight-flavor QCD on the lattice, *Phys. Rev. D* **89**, 111502 (2014).
- [80] T. Appelquist *et al.*, Strongly interacting dynamics and the search for new physics at the LHC, *Phys. Rev. D* **93**, 114514 (2016).
- [81] Y. Aoki *et al.* (LatKMI Collaboration), Light flavor-singlet scalars and walking signals in  $N_f = 8$  QCD on the lattice, *Phys. Rev. D* **96**, 014508 (2017).
- [82] A. D. Gasbarro and G. T. Fleming, Examining the low energy dynamics of walking gauge theory, *Proc. Sci., LATTICE2016* (2016) 242.
- [83] T. Appelquist *et al.* (Lattice Strong Dynamics Collaboration), Nonperturbative investigations of SU(3) gauge theory with eight dynamical flavors, *Phys. Rev. D* **99**, 014509 (2019).
- [84] Z. Fodor, K. Holland, J. Kuti, D. Negradi, C. Schroeder, and C. H. Wong, Can the nearly conformal sextet gauge model hide the Higgs impostor?, *Phys. Lett. B* **718**, 657 (2012).
- [85] Z. Fodor, K. Holland, J. Kuti, S. Mondal, D. Negradi, and C. H. Wong, Toward the minimal realization of a light composite Higgs, *Proc. Sci., LATTICE2014* (2014) 244.
- [86] Z. Fodor, K. Holland, J. Kuti, S. Mondal, D. Negradi, and C. H. Wong, Status of a minimal composite Higgs theory, *Proc. Sci., LATTICE2015* (2015) 219.
- [87] Z. Fodor, K. Holland, J. Kuti, D. Negradi, and C. H. Wong, The twelve-flavor  $\beta$ -function and dilaton tests of the sextet scalar, *EPJ Web Conf.* **175**, 08015 (2018).
- [88] Z. Fodor, K. Holland, J. Kuti, and C. H. Wong, Tantalizing dilaton tests from a near-conformal EFT, *Proc. Sci., LATTICE2018* (2019) 196.
- [89] Z. Fodor, K. Holland, J. Kuti, and C. H. Wong, Dilaton EFT from p-regime to RMT in the  $\epsilon$ -regime, *Proc. Sci., LATTICE2019* (2020) 246.
- [90] M. Golterman, E. T. Neil, and Y. Shamir, Application of dilaton chiral perturbation theory to  $N_f = 8, SU(3)$  spectral data, *Phys. Rev. D* **102**, 034515 (2020).
- [91] W. D. Goldberger and M. B. Wise, Modulus stabilization with bulk fields, *Phys. Rev. Lett.* **83**, 4922 (1999).

- [92] O. DeWolfe, D. Z. Freedman, S. S. Gubser, and A. Karch, Modeling the fifth-dimension with scalars and gravity, *Phys. Rev. D* **62**, 046008 (2000).
- [93] W. D. Goldberger and M. B. Wise, Phenomenology of a stabilized modulus, *Phys. Lett. B* **475**, 275 (2000).
- [94] C. Csaki, M. L. Graesser, and G. D. Kribs, Radion dynamics and electroweak physics, *Phys. Rev. D* **63**, 065002 (2001).
- [95] N. Arkani-Hamed, M. Porrati, and L. Randall, Holography and phenomenology, *J. High Energy Phys.* **08** (2001) 017.
- [96] R. Rattazzi and A. Zaffaroni, Comments on the holographic picture of the Randall-Sundrum model, *J. High Energy Phys.* **04** (2001) 021.
- [97] L. Kofman, J. Martin, and M. Peloso, Exact identification of the radion and its coupling to the observable sector, *Phys. Rev. D* **70**, 085015 (2004).
- [98] D. Elander and M. Piai, A composite light scalar, electroweak symmetry breaking and the recent LHC searches, *Nucl. Phys.* **B864**, 241 (2012).
- [99] D. Kutasov, J. Lin, and A. Parnachev, Holographic walking from tachyon DBI, *Nucl. Phys.* **B863**, 361 (2012).
- [100] R. Lawrance and M. Piai, Holographic technidilaton and LHC searches, *Int. J. Mod. Phys. A* **28**, 1350081 (2013).
- [101] D. Elander and M. Piai, The decay constant of the holographic techni-dilaton and the 125 GeV boson, *Nucl. Phys.* **B867**, 779 (2013).
- [102] M. Goykhman and A. Parnachev, S-parameter, technimesons, and phase transitions in holographic tachyon DBI models, *Phys. Rev. D* **87**, 026007 (2013).
- [103] N. Evans and K. Tuominen, Holographic modelling of a light technidilaton, *Phys. Rev. D* **87**, 086003 (2013).
- [104] E. Megias and O. Pujolas, Naturally light dilatons from nearly marginal deformations, *J. High Energy Phys.* **08** (2014) 081.
- [105] D. Elander, R. Lawrance, and M. Piai, Hyperscaling violation and electroweak symmetry breaking, *Nucl. Phys.* **B897**, 583 (2015).
- [106] D. Elander, C. Nunez, and M. Piai, A light scalar from walking solutions in gauge-string duality, *Phys. Lett. B* **686**, 64 (2010).
- [107] D. Elander and M. Piai, On the glueball spectrum of walking backgrounds from wrapped-D5 gravity duals, *Nucl. Phys.* **B871**, 164 (2013).
- [108] D. Elander, Light scalar from deformations of the Klebanov-Strassler background, *Phys. Rev. D* **91**, 126012 (2015).
- [109] D. Elander and M. Piai, Calculable mass hierarchies and a light dilaton from gravity duals, *Phys. Lett. B* **772**, 110 (2017).
- [110] D. Elander and M. Piai, Glueballs on the baryonic branch of Klebanov-Strassler: Dimensional deconstruction and a light scalar particle, *J. High Energy Phys.* **06** (2017) 003.
- [111] P. Candelas and X. C. de la Ossa, Comments on conifolds, *Nucl. Phys.* **B342**, 246 (1990).
- [112] A. H. Chamseddine and M. S. Volkov, NonAbelian BPS monopoles in  $N = 4$  gauged supergravity, *Phys. Rev. Lett.* **79**, 3343 (1997).
- [113] I. R. Klebanov and E. Witten, Superconformal field theory on three-branes at a Calabi-Yau singularity, *Nucl. Phys.* **B536**, 199 (1998).
- [114] I. R. Klebanov and M. J. Strassler, Supergravity and a confining gauge theory: Duality cascades and chi SB resolution of naked singularities, *J. High Energy Phys.* **08** (2000) 052.
- [115] J. M. Maldacena and C. Nunez, Towards the Large N Limit of Pure  $N = 1$  SuperYang-Mills, *Phys. Rev. Lett.* **86**, 588 (2001).
- [116] A. Butti, M. Grana, R. Minasian, M. Petrini, and A. Zaffaroni, The baryonic branch of Klebanov-Strassler solution: A supersymmetric family of SU(3) structure backgrounds, *J. High Energy Phys.* **03** (2005) 069.
- [117] C. Nunez, I. Papadimitriou, and M. Piai, Walking dynamics from string duals, *Int. J. Mod. Phys. A* **25**, 2837 (2010).
- [118] W. D. Goldberger, B. Grinstein, and W. Skiba, Distinguishing the Higgs boson from the dilaton at the Large Hadron Collider, *Phys. Rev. Lett.* **100**, 111802 (2008).
- [119] D. K. Hong, S. D. H. Hsu, and F. Sannino, Composite Higgs from higher representations, *Phys. Lett. B* **597**, 89 (2004).
- [120] D. D. Dietrich, F. Sannino, and K. Tuominen, Light composite Higgs from higher representations versus electroweak precision measurements: Predictions for CERN LHC, *Phys. Rev. D* **72**, 055001 (2005).
- [121] M. Hashimoto and K. Yamawaki, Techni-dilaton at conformal edge, *Phys. Rev. D* **83**, 015008 (2011).
- [122] T. Appelquist and Y. Bai, A light dilaton in walking gauge theories, *Phys. Rev. D* **82**, 071701 (2010).
- [123] L. Vecchi, Phenomenology of a light scalar: the dilaton, *Phys. Rev. D* **82**, 076009 (2010).
- [124] Z. Chacko and R. K. Mishra, Effective theory of a light dilaton, *Phys. Rev. D* **87**, 115006 (2013).
- [125] B. Bellazzini, C. Csaki, J. Hubisz, J. Serra, and J. Terning, A Higgslike dilaton, *Eur. Phys. J. C* **73**, 2333 (2013).
- [126] T. Abe, R. Kitano, Y. Konishi, K. y. Oda, J. Sato, and S. Sugiyama, Minimal dilaton model, *Phys. Rev. D* **86**, 115016 (2012).
- [127] E. Eichten, K. Lane, and A. Martin, A Higgs impostor in low-scale technicolor, *arXiv:1210.5462*.
- [128] B. Bellazzini, C. Csaki, J. Hubisz, J. Serra, and J. Terning, A naturally light dilaton and a small cosmological constant, *Eur. Phys. J. C* **74**, 2790 (2014).
- [129] P. Hernandez-Leon and L. Merlo, Distinguishing a Higgs-like dilaton scenario with a complete bosonic effective field theory basis, *Phys. Rev. D* **96**, 075008 (2017).
- [130] T. Appelquist, J. Ingoldby, and M. Piai, A Near-Conformal Composite Higgs Model, *Phys. Rev. Lett.* **126**, 191804 (2021).
- [131] D. Elander, M. Piai, and J. Roughley, Probing the holographic dilaton, *J. High Energy Phys.* **06** (2020) 177.
- [132] G. Aad *et al.* (ATLAS Collaboration), Observation of a new particle in the search for the Standard Model Higgs boson with the ATLAS detector at the LHC, *Phys. Lett. B* **716**, 1 (2012).
- [133] S. Chatrchyan *et al.* (CMS Collaboration), Observation of a new boson at a mass of 125 GeV with the CMS experiment at the LHC, *Phys. Lett. B* **716**, 30 (2012).
- [134] K. Pilch and N. P. Warner,  $N = 2$  supersymmetric RG flows and the IIB dilaton, *Nucl. Phys.* **B594**, 209 (2001).
- [135] M. Pernici, K. Pilch, and P. van Nieuwenhuizen, Gauged  $N = 8$   $D = 5$  supergravity, *Nucl. Phys.* **B259**, 460 (1985).

- [136] M. Gunaydin, L. J. Romans, and N. P. Warner, Gauged  $N = 8$  supergravity in five-dimensions, *Phys. Lett.* **154B**, 268 (1985).
- [137] M. Gunaydin, L. J. Romans, and N. P. Warner, Compact and noncompact gauged supergravity theories in five-dimensions, *Nucl. Phys.* **B272**, 598 (1986).
- [138] M. Gunaydin and N. Marcus, The spectrum of the  $S^5$  compactification of the chiral  $N = 2$ ,  $D = 10$  supergravity and the unitary supermultiplets of  $U(2,2/4)$ , *Classical Quant. Grav.* **2**, L11 (1985).
- [139] H. J. Kim, L. J. Romans, and P. van Nieuwenhuizen, The mass spectrum of chiral  $N = 2$   $D = 10$  supergravity on  $S^5$ , *Phys. Rev. D* **32**, 389 (1985).
- [140] K. Lee, C. Strickland-Constable, and D. Waldram, Spheres, generalised parallelisability and consistent truncations, *Fortschr. Phys.* **65**, 1700048 (2017).
- [141] A. Baguet, O. Hohm, and H. Samtleben, Consistent type IIB reductions to maximal 5D supergravity, *Phys. Rev. D* **92**, 065004 (2015).
- [142] O. Hohm and H. Samtleben, Exceptional field theory I:  $E_{6(6)}$  covariant form of M-theory and type IIB, *Phys. Rev. D* **89**, 066016 (2014).
- [143] A. Baguet, O. Hohm, and H. Samtleben,  $E_{6(6)}$  Exceptional field theory: Review and embedding of type IIB, *Proc. Sci., CORFU2014* (2015) 133 [arXiv:1506.01065].
- [144] M. Cvetič, H. Lu, C. N. Pope, A. Sadrzadeh, and T. A. Tran, Consistent  $SO(6)$  reduction of type IIB supergravity on  $S^5$ , *Nucl. Phys.* **B586**, 275 (2000).
- [145] I. Bakas and K. Sfetsos, States and curves of five-dimensional gauged supergravity, *Nucl. Phys.* **B573**, 768 (2000).
- [146] J. Distler and F. Zamora, Nonsupersymmetric conformal field theories from stable anti-de Sitter spaces, *Adv. Theor. Math. Phys.* **2**, 1405 (1998).
- [147] D. Z. Freedman, S. S. Gubser, K. Pilch, and N. P. Warner, Continuous distributions of D3-branes and gauged supergravity, *J. High Energy Phys.* **07** (2000) 038.
- [148] P. Kraus, F. Larsen, and S. P. Trivedi, The Coulomb branch of gauge theory from rotating branes, *J. High Energy Phys.* **03** (1999) 003.
- [149] M. Cvetič, S. S. Gubser, H. Lu, and C. N. Pope, Symmetric potentials of gauged supergravities in diverse dimensions and Coulomb branch of gauge theories, *Phys. Rev. D* **62**, 086003 (2000).
- [150] R. Hernandez, K. Sfetsos, and D. Zoakos, Gravity duals for the Coulomb branch of marginally deformed  $N = 4$  Yang-Mills, *J. High Energy Phys.* **03** (2006) 069.
- [151] A. Brandhuber and K. Sfetsos, Nonstandard compactifications with mass gaps and Newton's law, *J. High Energy Phys.* **10** (1999) 013.
- [152] M. Bianchi, O. DeWolfe, D. Z. Freedman, and K. Pilch, Anatomy of two holographic renormalization group flows, *J. High Energy Phys.* **01** (2001) 021.
- [153] I. Papadimitriou and K. Skenderis, Correlation functions in holographic RG flows, *J. High Energy Phys.* **10** (2004) 075.
- [154] A. Brandhuber and K. Sfetsos, Current correlators in the Coulomb branch of  $N = 4$  SYM, *J. High Energy Phys.* **12** (2000) 014.
- [155] A. Brandhuber and K. Sfetsos, Current correlators and AdS/CFT away from the conformal point, *arXiv:hep-th/0204193*.
- [156] K. Pilch and N. P. Warner,  $N = 1$  supersymmetric renormalization group flows from IIB supergravity, *Adv. Theor. Math. Phys.* **4**, 627 (2000).
- [157] A. Khavaev, K. Pilch, and N. P. Warner, New vacua of gauged  $N = 8$  supergravity in five-dimensions, *Phys. Lett. B* **487**, 14 (2000).
- [158] D. Z. Freedman, S. S. Gubser, K. Pilch, and N. P. Warner, Renormalization group flows from holography supersymmetry and a c theorem, *Adv. Theor. Math. Phys.* **3**, 363 (1999).
- [159] S. P. Kumar, D. Mateos, A. Paredes, and M. Piai, Towards holographic walking from  $N = 4$  super Yang-Mills, *J. High Energy Phys.* **05** (2011) 008.
- [160] D. Bak, A. Karch, and L. G. Yaffe, Debye screening in strongly coupled  $N = 4$  supersymmetric Yang-Mills plasma, *J. High Energy Phys.* **08** (2007) 049.
- [161] A. F. Faedo, M. Piai, and D. Schofield, Gauge/gravity dualities and bulk phase transitions, *Phys. Rev. D* **89**, 106001 (2014).
- [162] C. Csaki, J. Erlich, T. J. Hollowood, and J. Terning, Holographic RG and cosmology in theories with quasicalorized gravity, *Phys. Rev. D* **63**, 065019 (2001).